



Politecnico di Torino

Master's degree in Aerospace Engineering

A.A. 2022/2023

July 2023

Testing and characterization of Magnus effect modular wings for multirotor drones

Supervisors:

Prof. Domenic D'Ambrosio

Prof. Chrisophe Sicot

M. Matthieu Muschinowski

Candidate:

Alessandro Genoni

Acknowledgements

First, I would like to thank Prof. Christophe Sicot for his deep interest in this project and all the guidance and help during these six months. I want to thank as well M. François Paillé for his expertise and help with the wind tunnel and the test bench setup. I appreciate the ENSMA and Pprime staff for their participation in this project and the help with instruments and materials.

I would like to thank the Gipsa Lab in Grenoble for all the technical help and guidance and for all the testing equipment we were allowed to use. Without them, this project would not have been possible.

I would like especially to thank Jonathan Dumon for his devotion to the company and the project and for all the precious help in resolving many of the issues, especially in the beginning.

I would like to thank my supervisor at the Politecnico di Torino, prof. Domenic d'Ambrosio and the university in general for helping me become the engineer I always wanted to be.

I would like to remember prof. Elvio Bonisoli, that tragically passed away a few months ago. He supervised my Bachelor's degree and taught me a lot : many of the issues with mechanics, vibrations and manufacturing were solved thanks to his teachings.

Lastly, but not less important, I would like to sincerely thank the people of Chronics, Matthieu, Nicolas, and Raul, for truly welcoming me as part of the team and helping me grow and learn during this time together. Even if the start was a little bumpy, I feel fortunate to have found such an environment and great people.

Table of Contents

| | | |
|----------|--|-----------|
| 1 | Introduction | 1 |
| 1.1 | The company | 1 |
| 1.2 | The Magnus Effect and its history | 2 |
| 1.2.1 | Physics of the Magnus Effect | 2 |
| 1.2.2 | About CFD | 3 |
| 1.2.3 | History of the Magnus Effect | 3 |
| 1.3 | Applications | 4 |
| 2 | State of the art | 7 |
| 2.1 | Parameters and definitions | 7 |
| 2.2 | Influence of Reynolds number (Re_D) | 8 |
| 2.2.1 | Influence on the lift coefficient | 9 |
| 2.2.2 | Influence on the drag coefficient | 10 |
| 2.3 | Influence of aspect ratio (Λ) | 12 |
| 2.4 | Influence of end plate ratio (R) | 12 |
| 2.5 | Influence of Surface | 15 |
| 2.5.1 | Surface geometry | 15 |
| 2.5.2 | Surface roughness | 16 |
| 2.6 | Influence of velocity ratio (α) | 17 |
| 2.7 | Conclusion | 18 |
| 3 | Objectives of the project | 19 |
| 3.1 | Reproduction of existing data | 19 |
| 3.2 | Study of the aspect ratio Λ | 20 |
| 3.3 | Study of flow interactions | 20 |
| 3.4 | Determine polynomials for wings control | 21 |
| 4 | Test bench and data treatment | 22 |
| 4.1 | The wind tunnel | 22 |
| 4.2 | 3D printing | 23 |
| 4.2.1 | Design of the cylinders | 23 |
| 4.2.2 | Design of the test bench | 24 |
| 4.3 | Handling of the vibrations | 26 |

| | | |
|----------|---|-----------|
| 4.4 | Data acquisition | 26 |
| 4.4.1 | Load sensors and measuring chain | 26 |
| 4.4.2 | Analog reading and saving | 27 |
| 4.5 | Data treatment | 28 |
| 4.5.1 | General noise reduction | 28 |
| 4.5.2 | Detection of plateaux time segments for lift and drag calculation | 29 |
| 4.5.3 | Extraction of rotational speeds and calculation of the aerodynamic coefficients | 30 |
| 5 | Analysis of the results | 32 |
| 5.1 | Procedure to utilize data | 32 |
| 5.1.1 | Repeatability | 32 |
| 5.1.2 | Effect of Reynolds number (Re_D) | 33 |
| 5.1.3 | Presentation of the data | 34 |
| 5.2 | Effect of the aspect ratio (Λ) | 35 |
| 5.3 | Effect of end plate ratio (R) | 36 |
| 5.4 | Effects of the asymmetry | 38 |
| 5.5 | Effect of the plaque | 39 |
| 6 | Perspectives and critical points | 43 |
| 6.1 | Mechanics and setup | 43 |
| 6.1.1 | Design and vibrations | 43 |
| 6.1.2 | Manufacturing and 3D printing | 44 |
| 6.1.3 | Measuring chain | 44 |
| 6.2 | Aerodynamics | 44 |
| 6.2.1 | Anomalies and difficulties | 45 |
| 6.2.2 | Future development | 46 |
| 7 | Conclusion | 49 |
| A | Dampers test protocol | 50 |
| | Bibliography | 52 |

Chapter 1

Introduction

This work is the result of my final project at the ISAE ENSMA of Poitiers, where I spent two years thanks to a Double Degree program. This thesis was written as a report of my activities during a six months internship at Chronics Technologies in Grenoble. This work is a partnership between Chronics Technologies and the Institute Pprime in Poitiers. The project was conducted with the precious collaboration of the ISAE-ENSMA and the GIPSA Lab of Grenoble.

1.1 The company

The drone industry is experiencing a very steep growth with drones being more and more available to both professionals and consumers. The most common type of drone's architecture remains the multirotor approach: this family offers the ability to take off and land anywhere and the possibility to transport heavy loads easily. Unfortunately, this approach sacrifices flight endurance and range due to the globally high power consumption of such drones.

A lot of effort is being made to increase range and endurance of the aircraft: some have proposed, for example, a VTOL approach, with drones that can fly as planes and still land vertically, with the inconvenience of having a minimum speed required not to stall. Others have considered improving each component of the drone, thus reducing the consumption. Both these approaches, surely valid and interesting, lack the possibility to use an existing machine and improve its performances without rebuilding it completely.

It's with this in mind that Chronics Technologies was founded in May 2022. As a parts manufacturer, Chronics offer modular wings that can be added to an existing multirotor to optimize its power consumption without hindering its capacities. Utilizing the Magnus Effect, these wings are controllable, compact, and can be effective even at low speeds. These characteristics make them particularly interesting to application sectors such as delivery, agriculture and survey.

Born out of the Gipsa-Lab, where the company is still hosted, the start-up maintains a strong relationship with the academic sector, notably with the LEGI in

Grenoble, for the aerodynamic part, and ENSMA, for the aerodynamic tests and the supervision of this internship.

The company, being very young, is formed of three founders. I joined them as an aerodynamic specialist to help study the Magnus effect and its use in this domain. Among this small team, I had the opportunity to work on many different aspects, such as mechanics, 3D printing and flight testing.

1.2 The Magnus Effect and its history

1.2.1 Physics of the Magnus Effect

The Magnus effect is the generation of aerodynamic forces on a spinning body in a flow. The generation of lift is due to the difference of pressure on the sides of the body relative to the plane of the flow and this is derived from the friction on the surface that entertains the boundary layer.

The classical representation from the potential flow theory of a cylinder with circulation is well adapted to visualize this effect.

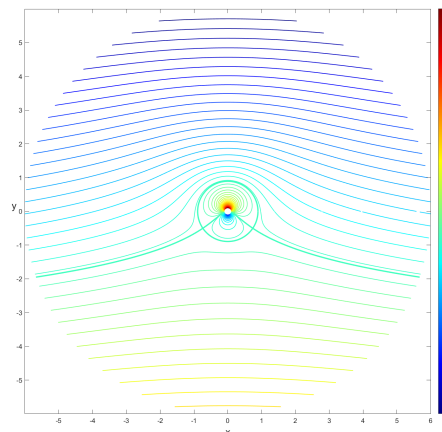


Figure 1.1: Simple potential visualization of the Magnus Effect. This representation is part of a previous course of basic aerodynamics and is made on MATLAB using a simple superposition of a constant stream, a dipole and a vortex that generates circulation.

In reality, the difference of pressure is due to the difference in speed induced by the propagation of the boundary layer from the cylinder to the flow. Thanks to the use of smoke and lasers, we were able to visualize the stream lines around a real spinning cylinder, as in picture 1.2.

A notable attempt at calculating an analytical formula for the aerodynamic coefficients was done by Swanson [1], followed by Badr [2]: but the many different variables, as shown in the following chapter, make the proposed solutions quite

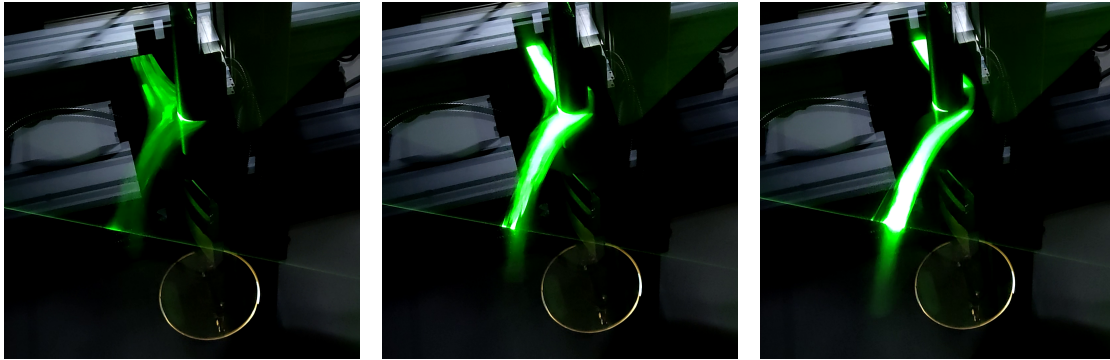


Figure 1.2: Stream line visualization in the wind tunnel

empirical and difficult to adapt to new situations. Overall, at the moment I could not find a suitable formula for said coefficients.

1.2.2 About CFD

The lack of experimental data makes validation of simulation of this phenomenon quite hard since one needs to take into account the state of surface and properly simulate turbulence. For example, the team at the Cranfield University followed the experimental studies realized by [3] with a numerical study [4] on the same subject and with the same conditions obtaining coherent trends but different values for drag and lift coefficients. The same was obtained by Elmiligui [5], where changing the type of simulation and the turbulence model changed the obtained coefficients for the same case. Zhang [6] also compared different models and obtained different results. Gowree and Prince, this last author of some of the most used experimental data in this document [3] [7], came to the conclusion that trends can be used but some effects remain visible only with some CFD approaches or experimental analysis.

In general, CFD is still very useful for visualizing the flow around the wing and it can predict, in some cases even precisely, the necessary coefficients in some specific cases. For the moment, considering the difficulty of such studies and the consequent necessity for experimental data, we opted for a fully experimental approach, leaving CFD for future development once enough data has been acquired.

1.2.3 History of the Magnus Effect

Gustav Magnus started his experiments in 1852 when he was professor of physics at the University of Berlin. He studied the behavior of a spinning cylinder in a flow but did not go as far as measuring the forces. In 1877, Rayleigh tried to explain the physics behind the motion of a tennis ball, but failed due to the absence of

sufficiently developed mathematical methods. In 1912 Lafay observed that with the spinning cylinder it was possible to obtain several times the lift of a conventional wing: he also studied the distribution of the stream lines and gave a first formula to calculate lift.

The first major attempt to use the Magnus effect came in the 1920's by Flettner, who proposed to replace the sails of a sailing boat with spinning cylinders. His idea was shared with Prandtl who proposed the addition of endplates: this increased the generated force by a relevant factor. Due to the poor reliability and the unpredictability of the Magnus effect at sea, those rotors were rarely used in commercial applications back then.

The majority of wind tunnel tests of the Magnus effect were conducted by Thom [8] and Reid [9] between the 20's and the 30's and then mostly abandoned for decades. Swanson [1] wrote a review in 1961 collecting the majority of the existing data and explaining the physics in detail.

Recently, with the increased attention to lower consumption for propulsion and the improved reliability of both mechanical parts and control systems, the Magnus effect is regaining some attention, especially in the aeronautic, maritime and energy production fields. Badalamenti and Prince [3] [10] [7] [4] [11] [12], lead the research on Magnus Effect and with other researches published several articles on the subject exploring new sides of the phenomenon and opening for new development.

1.3 Applications

As mentioned before, the Magnus Effect was very early proposed for maritime use: in this field it can act as a sail with better performances than a normal sail. The first applications started to appear in the 1920s thanks to the vision of Anton Flettner that fitted so called Flettner rotors on two ships, Barbara and Buckau (pictured in figure 1.3 on the left). Thanks to the researches of Borg [13], we know that Flettner claimed, after experimental tests, that his system could generate 8 to 10 times the force of equivalent surfaced sails with 4 to 5 the efficiency. It is important to note that sails technology was not the same as today's.

Despite the great success of the test on the two built ships, maybe, as Borg [13] hypothesizes, due to the wide availability of fossil fuels and the financial depression of the 1930s, the Flettner rotor for ships never caught the market and the idea was lost until much recent times.

Today, as the prices of fossil fuels is increasing and their availability greatly reducing, these applications are being revised as wind is once again considered a suitable propulsion method for cargo. For this, many designs or ideas are available and researches are being done to assess its feasibility on common oceanic routes. For this, the doctoral thesis of Bordogna [14] is a great source of data and experiments.

Remaining in the nautical domain, we can see Magnus effect being used as rudders or as fins to contrast currents. All of this applications are condensed in

the review of Borg [13] already cited.

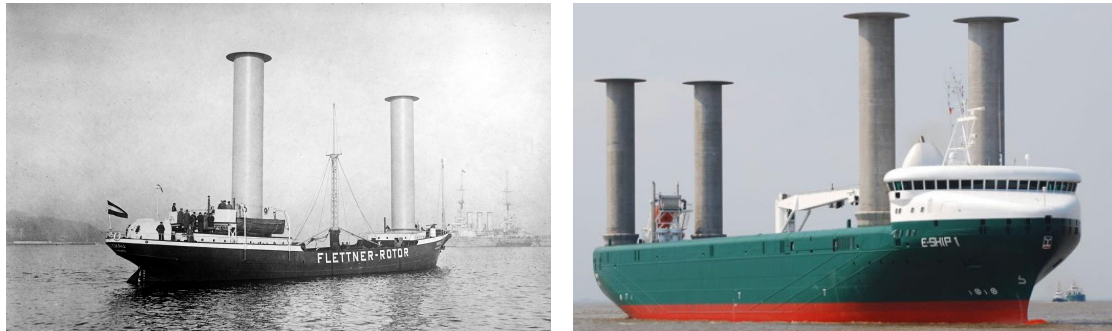


Figure 1.3: Historical and modern use of Flettner rotors on ships

In aeronautics the Magnus Effect has been introduced in many different applications. The first and most iconic use is as a wing substitute: this approach derived directly from the presentation of Flettner' Buckau and it consisted of a plane where the main wings had been swapped with cylinders. Unfortunately, this type of aircraft, following the consideration of Seifert [15], suffered from an unpropitious time were due to the end of World War I, most of the military development in many countries were at a stop. Furthermore, gyroscopic effects were encountered and the overall technology of the time did not allow for reliable operation of such a complicated system : differently from a normal plane or even a helicopter, in case of malfunction the lifting force ceases and there is no way to glide.

Another application can be seen at the leading or trailing edge of wings, in order to increase the performances without sacrificing safety and reliability. This allows for higher angles reducing the risk of stall or flow detachment. Prototypes of this technology were developed by NASA, that even managed to assemble a working aircraft, the NASA YOY-10. Extensive data on this subject was collected by Modi [16]. In figure 1.4 an example of the performances of such devices.

Some Magnus wing design are also capable of auto-rotation, removing the need for an actuator. However, the performances are clearly not the same and a lot of research is still missing on them. Some studies were conducted by Iversen [17] and Miller [18] concluding that the obtained velocity ratio are very low and thus suitable for very limited applications. This subject is very interesting for the Company, but unfortunately falls outside of the scope of this work.

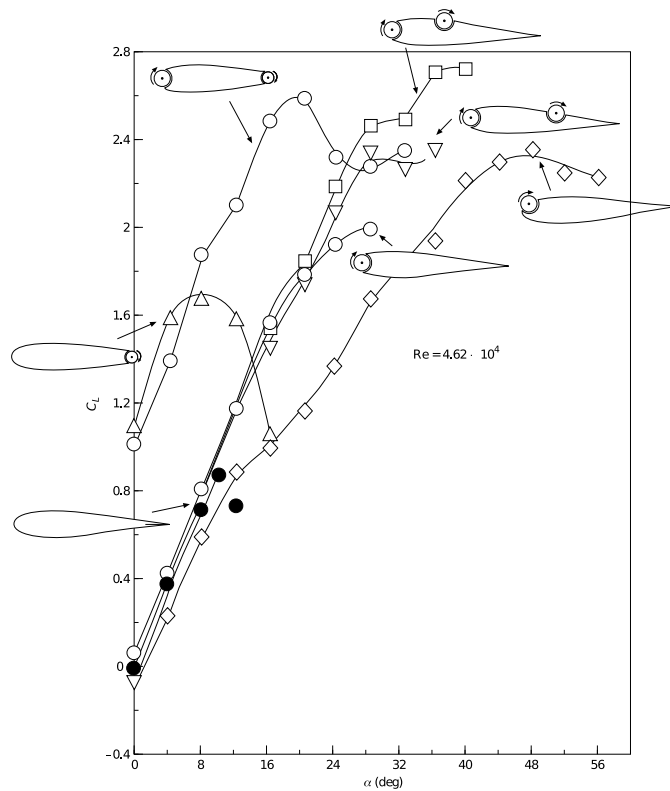


Figure 1.4: C_L over angle of attack for wings with integrated spinning cylinders

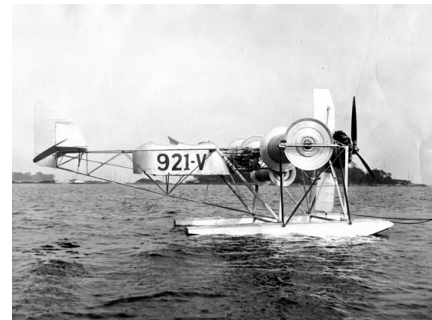


Figure 1.5: The Plymouth A-A-2004 with Magnus effect wings



Figure 1.6: NASA YOV-10A prototype with an integrated rotating cylinder flap

Chapter 2

State of the art

This chapter aims to summarize the data collected from various articles and previous works. All the data will be sorted according to the different parameters in order to understand the importance and influence of the most relevant variables and the accordance between all the different authors and experiments.

Jost Seifert published in 2012 a paper [15] in which various aspects of the Magnus effect were discussed. He gathered a lot of data from different publications, some aimed at different objectives but still relevant. Some documents are only found in German, making their use difficult in this discussion. My work will be compared with the relevant parts of Seifert's review of the Magnus effect literature.

2.1 Parameters and definitions

The most important parameter that controls cylindrical Magnus effect wings is the ratio between the local tangential velocity and the velocity of the flow. We will call this velocity ratio (α). Its effect is similar to the angle of attack of a classic wing. Where ω is the rotational speed in rad/s and r the radius in m , velocity ratio is defined as:

$$\alpha = \frac{\omega \cdot r}{V_{\infty}}$$

Another important parameter, similarly to classic airfoil wings, is the dependency on the velocity of the flow and size of the object. I will approach this based on the Reynolds number (Re_D) calculated using the diameter of the cylinder as the characteristic length of the flow.

$$Re_D = \frac{V_{\infty} \cdot D}{\nu}$$

The third parameter I will study is the aspect ratio (Λ) of the cylinder calculated as the ratio between length and diameter. This parameter, as in regular wings, has

a major impact on the efficiency of the wing. Unfortunately, in the context of this work, its study will be limited in range due to installation and structural needs.

$$\Lambda = \frac{L}{D}$$

Following, I will approach the influence of end plates and its sizes on the cylinder. This will be approached using the end plate ratio (R) defined as the ratio between the end plate diameter and the diameter of the cylinder.

$$R = \frac{D_{disk}}{D_{cyl}}$$

Finally, I will discuss, at least qualitatively, the influence of the surface in terms of roughness and geometry.

In order to have comparable data for later use, the results will be presented using aerodynamic coefficients such as lift coefficient (C_L), drag coefficient (C_D) and efficiency. These coefficients are defined as follows :

$$C_L = \frac{2 \cdot L}{\rho \cdot V_\infty^2 \cdot S} \quad C_D = \frac{2 \cdot D}{\rho \cdot V_\infty^2 \cdot S} \quad e = \frac{L}{D} = \frac{C_L}{C_D}$$

where L and D are lift and drag forces respectively.

2.2 Influence of Reynolds number (Re_D)

This parameter has been studied by Badalamenti [3] and Prince [7] in their work on the Magnus effect. Even if the study of the mentioned researchers is aimed at specific parameters, each of these papers start with a comparison of the baseline with previous results, notably from the work of Thom [8], Betz [19], Reid [9] and Swanson [1].

Direct and autonomous comparison between datasets is complicated due to the absence of raw data : while Thom [8] and Reid [9] provide most of their data, Badalamenti[3] and Prince [7], even upon request, did not provide their data and results had to be extrapolated directly from the graphs in the papers.

The influence of the Reynolds number can also be extracted from other experiments where the speed is indicated, regardless of the studied configurations, for example from Prince's paper on the influence of surface texture and geometry [7].

It has to be noted that the baseline results are based on cylinders with mostly unknown surface finish, apart from Badalamenti [3] and Prince [7]: due to the complex nature of the Magnus effect some anomalies are to be expected.

The results presented in this section try to correlate Re_D to C_L and C_D , always functions of α .

2.2.1 Influence on the lift coefficient

In order to understand the correlations, we need to distinguish three regions based on the velocity ratio: α less than 1, α more than 2.5 and the region in between. This distinction is based on the behavior of the lift coefficient that tends to be linear in the central region.

Velocity ratio less than 1

If α is less than 1, at higher Reynolds number, we might encounter a phenomenon of inversion of the Magnus effect, generating less lift than expected or even generating negative lift in the worst cases. This phenomenon is most evident in the work of Swanson [1] studied by Prince [7] and reported in figure 2.1. This can be influenced by the different texture or different test conditions. In any case, there is a general agreement that this inversion can occur in this range, specifically with higher Re_D .

Swanson [1] and Thom [8] suggest, as reported by Seifert [15] that this inversion of the lift force, that can induce a coefficient up to $C_L = -0.6$, could be due to position of the transition points on the sides of the rotating cylinder, where the laminar flow either turns to turbulent flow or separates. Thom [8] also observed that the inversion is surface dependent and was observed only in specific configurations and with a few specific surface roughness.

More on this subject can be found in the work of Krahn [20], who suggests a set of requirement on the flow for this phenomenon to happen.

A similar result can be seen in the baseline test of Badalamenti [3] in figure 2.2, highlighting the influence of the Reynolds number on the inversion of Magnus effect. The data shows a clear diversion of the lift coefficient with the two highest Reynolds numbers.

Figures 2.1 and 2.2 both study a limited range of Reynolds, but this range is the most interesting for our applications and is easy to reproduce in our available wind tunnel and directly on the drones. For this work, a wider range of Reynolds was deemed not necessary.

Velocity ratio between 1 and 2.5

In this region, there is a general agreement between authors that the lift coefficient is independent of Reynolds number. This can easily be seen in figure 2.2. The same conclusions can be taken from figure 2.3 and from the work of Reid [9] in figure 2.4.

In this range, the slope, as shown by Seifert [15], depends slightly on the surface finish and the Re_D . Overall at this stage it is difficult to determine a law that correlates the slope with different Reynolds.

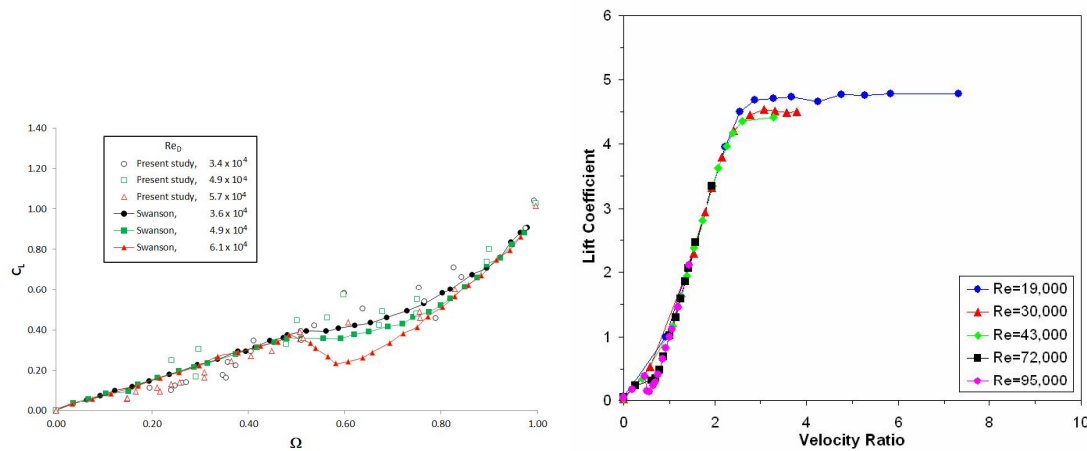


Figure 2.1: Influence of Re_D on C_L , from Prince [7]

Figure 2.2: Influence of Re_D on C_L , from Badalamenti [3]

Velocity ratio greater than 2.5

The work of Badalamenti [3] suggests that at higher velocity ratios there is a dependency on the Reynolds number. It is possible to note in figure 2.3 that, with lower Re_D , the limit of the lift coefficient seems to be higher. This same result is shown partially in figure 2.4 with a limited set of data. On the contrary, Swanson [1] does not seem to observe a similar behavior.

2.2.2 Influence on the drag coefficient

When for the lift coefficient the results are consistent and coherent throughout the different sources, the same cannot be said about the drag coefficient. It is important to note that the measure of this coefficient is by itself more dependent on external factors and the way the cylinders are fabricated. Another major factor on this parameter is the state of the surface that affects boundary layer transition and separation.

One element that deeply affects the drag, as noted by Prince [7], is the vibration of the experiment. An increased vibratory state could determine a premature detachment of the boundary layer transforming the flow from laminar to turbulent with a consequent change in the drag coefficient. At higher rotational speeds most of the experiments self-stabilize and thus prevent vibrations from affecting the transition of the flow.

As seen in figure 2.5, we can observe that data from Prince [7] show an increase of drag in a specific region. This phenomenon is not observed by Swanson [1] (compared directly in figure 2.5) nor by Badalamenti [3]. Prince suggests that this is related to the vibration phenomena mentioned above and should be considered

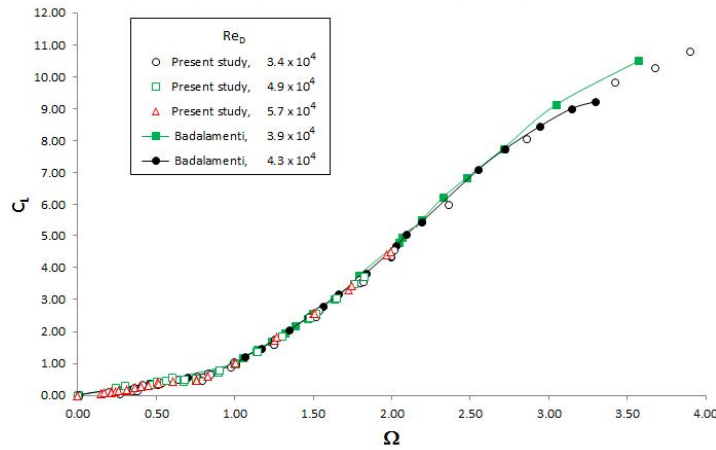


Figure 2.3: Influence of Re_D on C_L , from Prince [7]

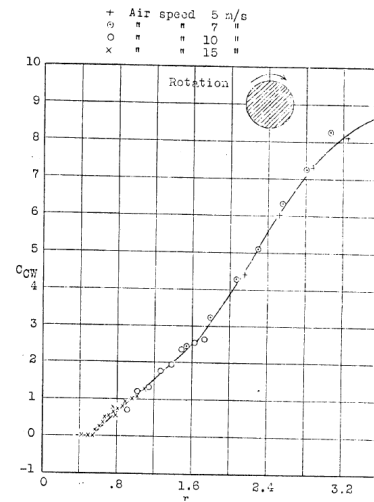


Figure 2.4: Influence of Re_D (in the form of velocity) on C_L , from Reid [9]

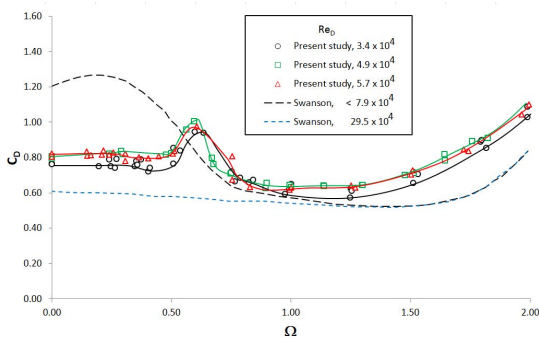


Figure 2.5: Influence of Re_D on C_D , from Prince [7]

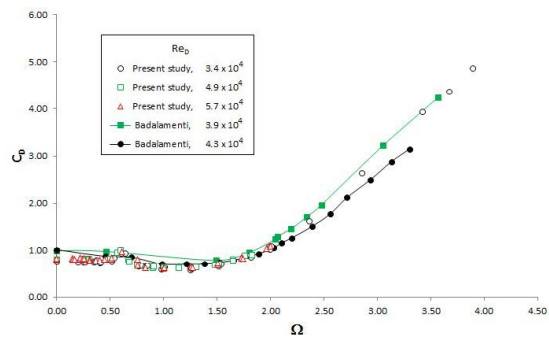


Figure 2.6: Influence of Re_D on C_D , from Prince [7]

an anomaly. Unfortunately, there is not enough data to validate this assumption, mostly because this region is not of practical interest.

Most of the results, independently of the test conditions, show an initial decrease and a subsequent increase of drag. This can be seen in most of the plots from Badalamenti [3] that will be shown later.

The actual influence of the Reynolds number on the drag coefficient is hard to study due to the limited data available. For example, Badalamenti [3] did not even differentiate in his work the Re_D of the different tests due to the low influence of this parameter. Nevertheless, from figure 2.6 we can assume that lower Re_D

corresponds to slightly higher drag, especially at higher velocity ratios, but the influence seems to remain limited.

2.3 Influence of aspect ratio (Λ)

The data I could find on aspect ratio is a direct comparison made by Badalamenti [3] in the initial phase of his work: the author compares results from different papers and tries to draw conclusions. This data considers cylinders without endplates.

We can see from figure 2.7 that at aspect ratios below 10 we can expect a stagnation of the lift force in what we consider a plateau. For higher aspect ratios, the lift force seems to continue to increase changing slope without reaching a plateau. For our applications we can assume that lift force will develop a plateau.

We can also observe that there is an important range of α where the lift coefficient is largely independent of the aspect ratio and its behavior, similarly to regular wings, can be considered linear.

The influence of the aspect ratio, noted by Badalamenti as A , on the lift coefficient at high Λ is clear. It is possible to deduce that to higher aspect ratios corresponds a higher obtainable lift coefficient, practically reaching the plateau at higher velocity ratios or even continuing to increase the generated lift. The two contrasting examples of lowest and highest aspect ratios clearly highlight this pattern.

It is important to note that in this comparison the reference surface, defined as diameter multiplied by the length $S = D * L$, is not constant thus showing, at first approximation, an independence of the actual size of the wing from its performance.

The discussion about drag is more complex. As shown in figure 2.8, there is no evident correlation between drag and aspect ratio. This is not due, in my opinion, to a physical phenomenon, but to the lack of exhaustive data and the fact that drag is more difficult to measure. Drag is in fact very easily modified by other factors such as the texture.

On this topic I would agree with Badalamenti's [3] conclusions and assume that, from this data, it is not possible to extract a correlation between drag generation and aspect ratio. One interesting aspect of this comparison is the discrepancy between Swanson's [1] results in the 2D approximation, noted as Ref.9 in the graph, and experimental data from Badalamenti and others.

2.4 Influence of end plate ratio (R)

The influence of this parameter has been deeply studied by Badalamenti [3]. He conducted tests ranging R from 1 (no plates) to 3. I will summarize the results and invite to read the original article for further details.

We can clearly see in figure 2.9 that the presence of end plates delays the formation for the plateau of the lift coefficient. From figure 2.10 we can quantify

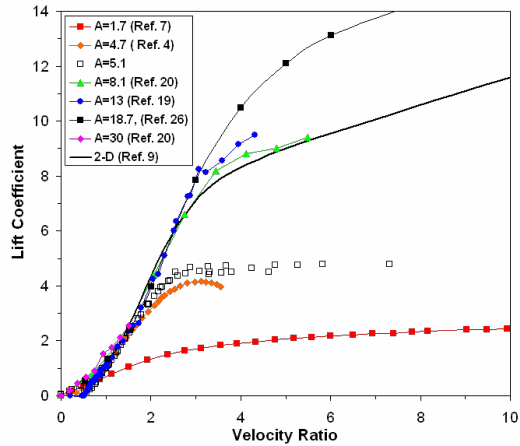


Figure 2.7: Influence of λ on C_L , from Badalamenti [3]

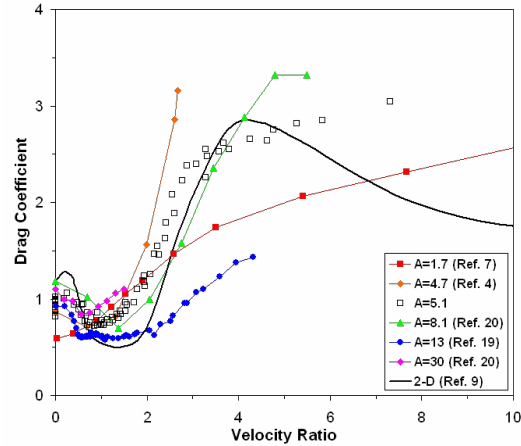


Figure 2.8: Influence of λ on C_D , from Badalamenti [3]

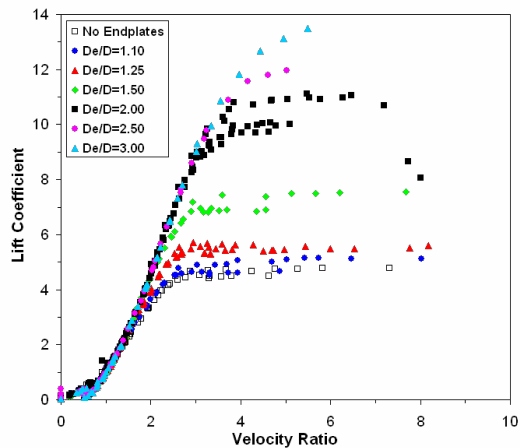


Figure 2.9: Influence of R on C_L , from Badalamenti [3]

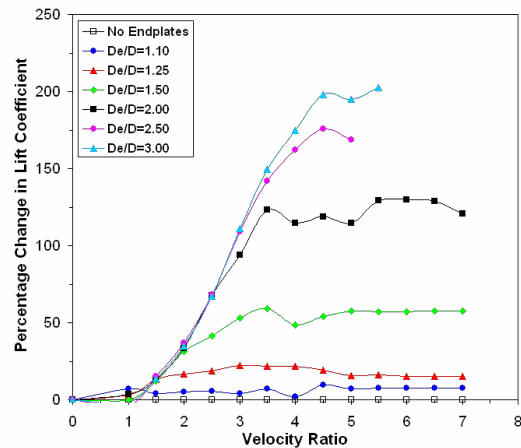


Figure 2.10: Percentual variation of C_L in function of R, from Badalamenti [3]

that effect of the end plates with gains of lift up to more than 200%. Badalamenti suggests that the gain in lift is directly proportional to the R factor: he gives the hypothesis that the gain is:

$$\text{Gain} = (R - 1) * 100 \%$$

It appears that the presence of end plates, similar to the winglets on a classic wing, acts as an artificial way of increasing the aspect ratio: the behavior we observe is similar to that of an increased λ . We can remark that the effect of the endplates

is relevant only at velocity ratios greater than 2. Before that, no major effect is registered.

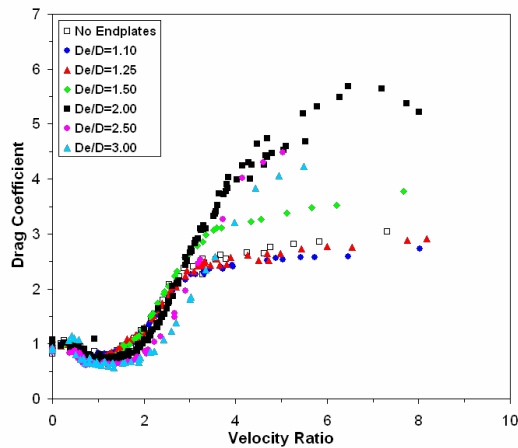


Figure 2.11: Influence of R on C_D , from Badalamenti [3]

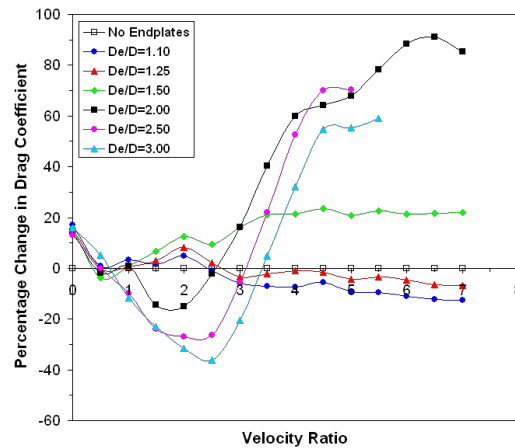


Figure 2.12: Percentual variation of C_D in function of R, from Badalamenti [3]

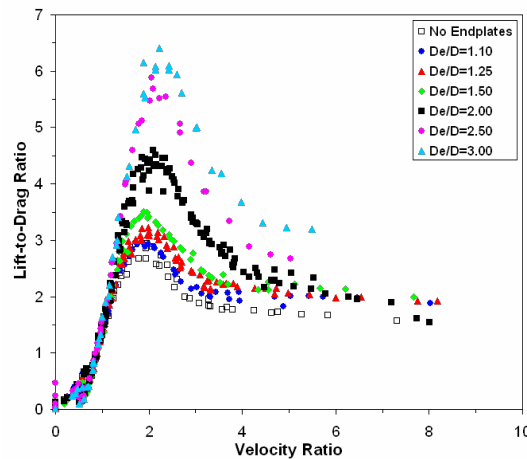


Figure 2.13: Influence of R on the efficiency, from Badalamenti [3]

A similar behaviour seems to be obtained for the drag coefficient, as shown in figure 2.11. An increase of R shows a delayed plateau of the drag coefficient. If we observe figure 2.12 we can see that the increase in drag is largely inferior to the increase of lift. This can be seen as well in figure 2.13. Also, differently as what was noted for the lift coefficient, the drag coefficient is dependent on R in the lower end of values and decreases for velocity ratios less than 2.

If we observe the curve of the aerodynamic efficiency we can see that it increases with the ratio of the endplates. The position of its maximum depends on the size of the endplates. We can assume that, at least for the range measured, higher R equals better performances. It is also evident that the choice of the size of the endplates depends on the functioning point of the wing or vice versa.

In any case, it appears that the most efficient velocity ratio is around 2 for the measured values. Changing the aspect ratio could influence these results since the aerodynamic effect of the two parameters is similar.

2.5 Influence of Surface

The study of the surface is divided in two macro areas: surface geometry and surface roughness.

2.5.1 Surface geometry

Surface geometry was investigated already by Reid [9], who tested a cross-shaped rotating wing, and later by Prince [7].

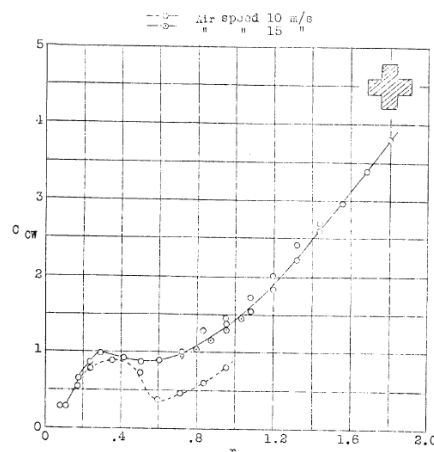


Fig.8 Cross cylinder.

Figure 2.14: C_L over α of the cross cylinder, from Reid [9]

Reid, as shown in figure 2.14, obtained a slight increase of lift in the linear region of α compared to his experiment on the simple cylinder in figure 2.4. It has to be noted that Reid's interest was not to find any optimized shape. Data show that, together with the increase of lift, the power needed to spin the cylinder also increases, but with a much higher rate.

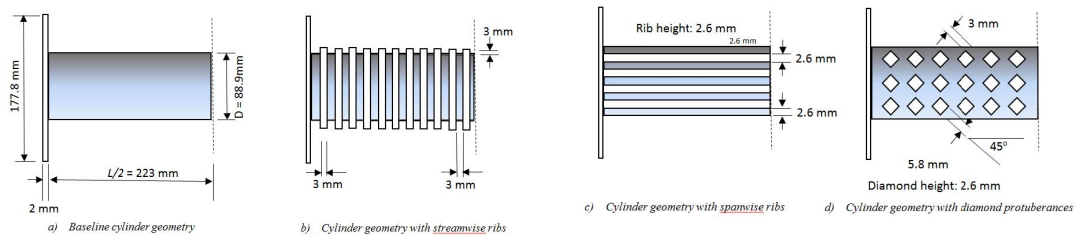


Figure 2.15: Prince's set of cylinders, from Prince [7]

A different approach was taken by Prince in his work [7] dedicated to the influence of geometry on the aerodynamic forces. He compared three different geometries, as per figure 2.15. The test found that certain geometries, as shown in figure 2.16, in this case spanwise ribs, increase the lift coefficient and the drag to lift ratio making the wings more effective, while some other geometries can negatively affect the performances of the wing.

One geometry of high interest is the diamond shaped protuberances: the effect of this configuration is forcing the boundary layer to become turbulent thus obtaining the post-critical results in any circumstance.

Unfortunately, no data regarding power consumption is available and we cannot determine, for practical uses, if the slight increase in efficiency and lift is worth a possible change in power consumption.

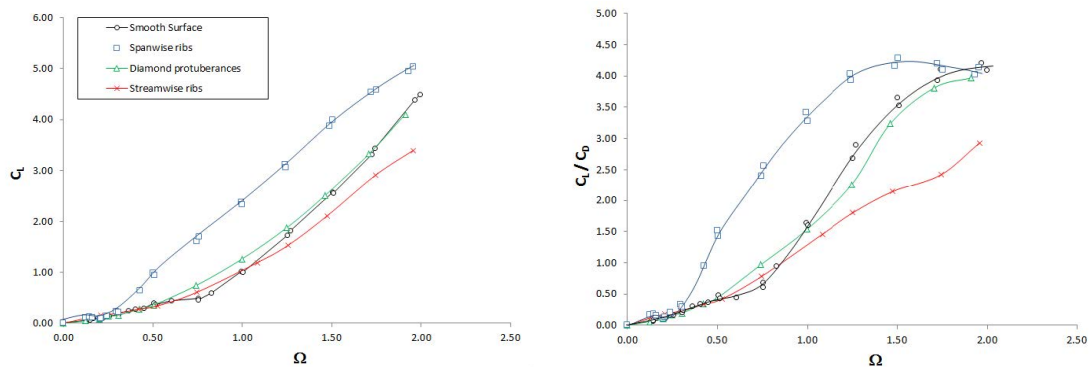


Figure 2.16: Prince's set of cylinders, from Prince [7]

2.5.2 Surface roughness

Data regarding this parameter is old and largely incomplete. Thom [8], as reported by Seifert [15], studied the influence of the surface finish in his work but failed to mention any value of roughness of the surface. He used a wooden cylinder and a cylinder to which he attached sand on the surface to make it rough.

Seifert [15] also reports that the drag coefficient increases with the surface roughness, but does not provide quantitative data on the matter, nor on the aerodynamic efficiency. As in many other parameters, the most relevant change is in the regions of low and high α .

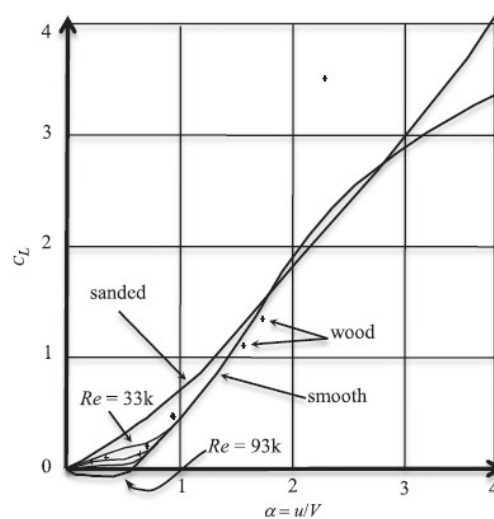


Figure 2.17: Influence of the surface finish on C_L , from Seifert [15] that includes data from Thom [8]

2.6 Influence of velocity ratio (α)

We observed from all data presented so far that the influence of the velocity ratio behaves very similarly to the angle of attack of any regular wing. As like in any regular wing, rotating cylinders differ in behavior accordingly to the parameters we previously introduced. The influence of this parameter thus depends on too many factors to be described precisely here.

The main difference between this parameter and the angle of attack of an airfoil is that it can be easily changed and adapted to different situations. This makes the α a versatile variable to be adapted to the proper scenario and wing geometry.

In any case, some recurring effects can be seen. We can spot a plateau in both lift and drag traces at high velocity ratios (α greater than 2.5) and a variable behavior in the region of α smaller than 1. In the region in between, lift is mostly linear following different curves according to the factors discussed, and the drag coefficient is quadratic, similarly to regular airfoils. All of these behaviors are captured, for example, in figures 2.9 and 2.11.

2.7 Conclusion

Data gathered on the Magnus effect is varied and results from different data collection methods. This makes its analysis complicated and for some aspects also unreliable. We could observe, even in modern works, that even a small setup problem can affect the results and provide incoherent data. In Prince's case [7], for example, vibrations changed the drag behavior thus making the results unreliable at least in the lower range of α .

Nevertheless, we could assume that the effect of some variables is sufficiently understood, like the behavior of endplates ($R < 3$), while some remain uncertain, like surface roughness or the real effect behavior at low velocity ratios ($\alpha < 1$) where research is incomplete.

As mentioned, there are a lot of variables, and some, like the size of the cylinder (measured as surface), were not even discussed due to the lack of data available. It would be very time consuming to fully analyze every aspect and its effect on every other parameter: for this reason a more specific approach, targeting one parameter at a time or a pair of parameters, could be the best option to study this interesting phenomenon.

Where data seems to be less precise is in the measure of drag. In order to study practical applications of this type of wings, this parameter should be better understood and a model to predict it, at least to some extent, should be available for different classes of cylinders. The same applies to the torque (or power) needed to rotate the cylinders.

Unfortunately, it is also difficult to define what a "class" of these cylinders is, as changing one parameter could potentially, in unpredictable ways, affect the other parameters.

Chapter 3

Objectives of the project

As seen in the previous chapter many parameters need further studying and understanding. Together with the company, we decided on a list of areas to explore that could conjugate the needs of the product and those of the research.

We opted to set a scale suitable for our current generation of prototypes and we prioritized certain aspects, while still allowing to test things that are purely for research purposes, such as high α . The analysis of some parameters, such as a better understating of the aspect ratio and the combined effect of Λ and R , is completely absent in the literature and its knowledge is vital for the design of the products.

Considering the lack of satisfying datasets and considering the complex nature of the phenomenon, we decided to adopt a fully experimental approach testing everything in the wind tunnel. This had never been done by the company and had to be fully developed, both in the objectives and the means, especially mechanically. The following chapter is entirely dedicated to the setup.

3.1 Reproduction of existing data

The first objective we decided to pursue was the reproduction of existing data, especially from Badalamenti [3] since their work is the most recent and better documented. We accepted the fact that it would be impossible to reproduce at the same scale, but we respected the same geometry. Badalamenti used quite a large cylinder with a very smooth surface. We have a small cylinder with rougher surface and thus we expect some differences in the results.

Similarly to every new test campaign, this phase is important to be able to compare the differences with the literature and better understand the impact of the test bench on the results. We opted to try to reproduce as many tests as possible and check if the magnitude of the coefficients was the same. The literature also provides global trends that we hope to respect and find in our data.

Considering that this had never been done before by this company, we had to make sure that all of the sensors, instruments and processes were acceptable

to properly read and treat data. It is important to be able to predict the different phenomena in order to properly set up the system and prepare for the tests. This is treated deeply in chapter 4

3.2 Study of the aspect ratio Λ

The most important variable for which dedicated research is missing from the literature is the aspect ratio, even though it is incidentally the most important in the definition of the geometry of the wing.

We decided to try a range of aspect ratios from 5 to 10, considering that this range allows to be easily mounted and manufactured. We decided to test the aspect ratio of 5.1, that corresponds to the value used by Badalamenti and Prince, in order to reproduce the same tests.

Similarly to regular wings, and based on the literature, we expected to see an increase in the efficiency of the wings with Λ . The increase should tend to the ideal symmetrical configuration, but we did not expect to get close to the 2D ideal case, even at the highest chosen aspect ratio.

We also decided to test different sizes of diameter and speeds with same aspect ratio, in order to test the effects of Reynolds number, that we hope, based on the literature, to be negligible at least within the chosen values.

As shown in the literature, the end disks, as per the end plate ratio, play a similar role as the aspect ratio. We decided to test different sizes of disks, ranging from 2 to 3 times the diameter. This was decided considering structural and manufacturing limitations of larger disks and from the literature, that shows a very positive impact of disks in this range.

The combined effect of R and Λ was studied. We expected a similar and combined effect of larger disks and longer wings, but we still wanted to explore and understand the weight of each variable on the performances. A particular interest is on the possibility that an increase of the end plate ratio in conjunction with higher aspect ratio would result in a negligible effect on the performances

3.3 Study of flow interactions

We decided to begin the tests with what we called a symmetrical approach, that consists in trying to have a full symmetry on both sides of the cylinder. In order to do this we installed similar fairings on both sides of the cylinder. We started with this configuration in order to establish a reference point for further configurations and to be able to compare the results with other publications.

As a second step, we proceeded removing the symmetry and leaving one end of the cylinder completely exposed to the flow. We expected a decrease of the overall performances, but did not know by how much and if some of the others parameters affected this. This configuration is similar to that of a real life application of this wings on drones, where one side is not attached.

We concluded with testing a third configuration, with one end of the cylinder in a boundary layer, thus simulating the presence of the body of a bigger aircraft where the wing would be mounted on or maritime applications, where the ship can be represented as a flat surface. We opted to test a plate of appropriate size mounted very close to the end disk. We expected to have a reduction of the importance of the end disk in the boundary layer and thus a further reduction of the performances of the wing. All of the configurations are represented in figure 3.1

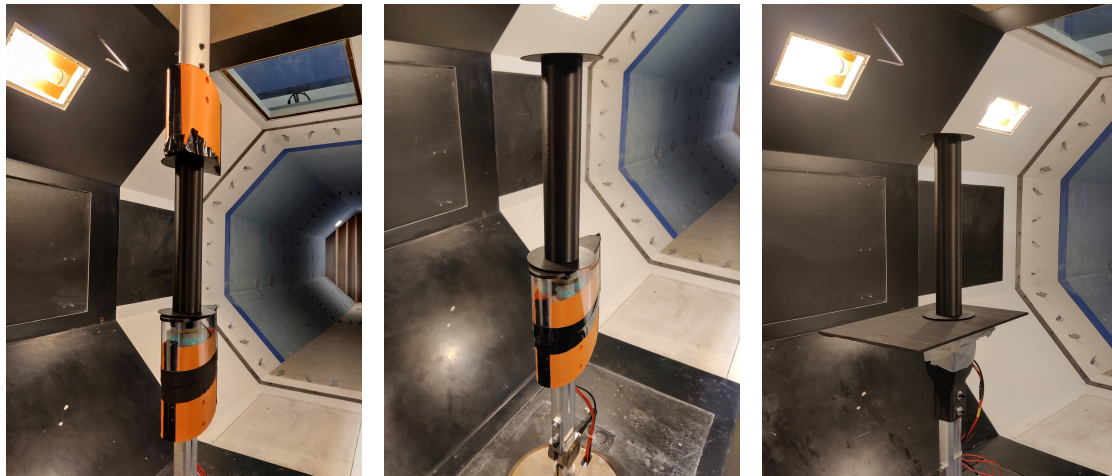


Figure 3.1: Symmetrical, asymmetrical and boundary layer configuration

3.4 Determine polynomials for wings control

In these tests we will aim at interpolating the obtained curves that will have a direct impact on our product and demonstrators development.

The polynomials interpolated for each configurations will be used to predict the effect of such wings on the drones and to determine pertinent dimensions for wings in order to obtain the desired increases in flight time and distance.

Another important application is in the embedded code of the drones mounting Magnus effect wings, as it is important to estimate the aerodynamic forces on the wings in order to be able to control the α during flight.

On a secondary level, knowing the forces on the wings and on the entire aircraft, we could determine the aerodynamic forces on the chassis: this would allow for real life conditions tests on the wings and faster prototyping without the use of a wind tunnel.

Some flight tests are already planned to compare the wind tunnel models to real flight results, and there will be a constant back and forth between these two test procedures in the future.

Chapter 4

Test bench and data treatment

As mentioned before, no previous attempt to such a test campaign was done by the company and everything had to be studied and adapted. A major part of my internship was hence spent on the mechanical and technical development of the test bench.

The test campaign was split in two parts, with one week of tests in July and one in October. The first round of test was essential to understand and address the problems that we encountered and many upgrades were done for the second round.

4.1 The wind tunnel

Thanks to our partnership with professor Christophe Sicot of the Institut Pprime of Poitiers, who supervised this work during my internship, we got the opportunity to rent the S120 wind tunnel of the ENSMA, located in Poitiers. This wind tunnel has an octagonal test section of $1.2m^2$ that is well suited to the size of our models. The help and guidance of François Paillé, the engineer in charge of the platform, were crucial in our understanding and ability to properly extract the data we wanted from the setup.

The wind tunnel allows for tests in the range of 5 to $80m/s$, but we generally opted to stay in the range of 5 to $20m/s$. Higher speeds would have required rotational speeds impossible to reach with our motors in order to obtain the desired values of α , and this range of values is the most interesting for the practical applications in the product.

The setup of the wind tunnel provided measurement of dynamic pressure, static pressure and temperature. These were processed to obtain density and velocity of the flow. These parameters allow to determine the freestream conditions.

We considered this wind tunnel appropriate to our test situation since the size of the wings allow for a sufficient distance from the walls and the overall bench: in the worst possible condition of $\Lambda = 8$ and $D = 50mm$, the solid blockage is close to

5%. Nevertheless, we observed a fluctuation of the freestream airspeed at higher rotational speeds, that was taken into account during the analysis of data.

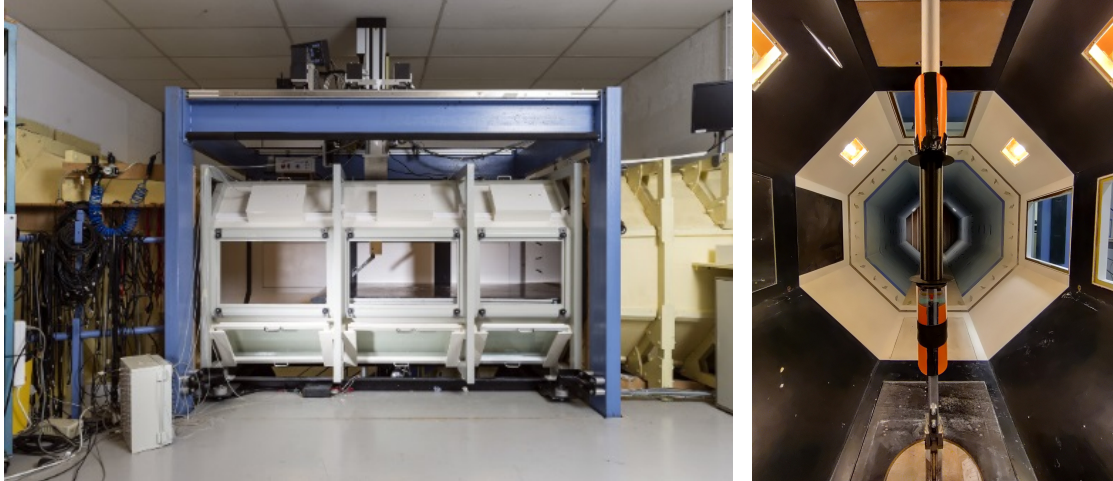


Figure 4.1: The test section of the S120 wind tunnel

4.2 3D printing

The company uses 3D printing for the majority of mechanical parts and pieces. As part of my internship I took care of revamping the design and production of the wings as well as putting the test bench together. Every piece was custom made and printed in-house on the many printers of Chronics, that I learned how to use, tune and maintain.

4.2.1 Design of the cylinders

The shape of the wings is clearly quite easy to design and the difficulty lies in the production and operation of such wings. On one side, one has to guarantee that the quality is always above a certain standard, assuring a reliable manufacturing and a precise concentricity for stable operation. On the other side we had to make sure the cylinders were sufficiently easy and quick to print in order to accept and mitigate print or operating failures.

For this, I opted for a modular approach, printing separately the two end disks, one with the motor housing, and the cylinder. Every setup is then formed of three independent parts that can be swapped and replaced if needed. This, even if mechanically more challenging, allows to reduce the overall manufacturing time and allows to, for example, change the type of motor without reprinting the whole setup. In this case we pass from 8+ hours of printing to just 40 minutes.

The biggest mechanical challenge was the mechanical coupling of the cylinder and its base. The cylinders are designed to spin at speeds up to $18000rpm$, which is not an easy task. For this, I opted for a conical shape on the top that would help with the centering and grooves on the side to transmit torque. The motor transmits torque to the base by friction: tolerances were an essential part of the tuning process. The shaft of the motor is then used to tighten the system and lock everything into place.

For the first round of tests I opted for a lower angle in order to facilitate the printing of the cylinders: this system turned out to be not sufficient at higher speeds and overall impacted the ease of printing of the cylinders. The system was completely redesigned in August with a steeper angle of 45 degrees and a bi-conical shape that allows to screw in motors with regular shafts.

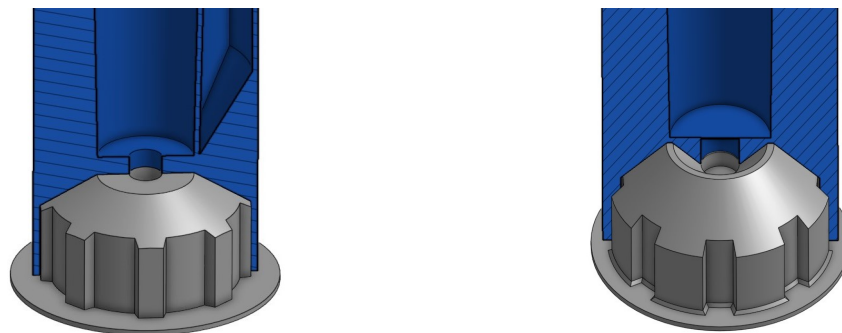


Figure 4.2: First and second version of the wings' mount

4.2.2 Design of the test bench

When I started designing the test bench, I had some requirements that were mostly the ease of use and the ease of change of the test wing. This was specifically important in the case of longer cylinders that would not have permitted to be screwed in without the disassembly of the top part of the wind tunnel

For the first round of tests, I tried to produce a simple mount for the motor that could be unmounted without the use of tools and in a rapid way (figure 4.3 in the middle). This "fast mount" was a failure and instead a simpler and more solid mount was used (figure 4.3 on the left). Using this approach, it was often needed to unscrew the part from the load sensor after having unmounted the cylinder. This was a very cumbersome process that negatively impacted the quantity of the tests and that was addressed for the second round in October.

The second version of the fast mount was developed by the company's mechanical engineer and was a big improvement, as it allowed for rapid exchange of the cylinders without the need of disassembly in the tunnel itself. This improvement

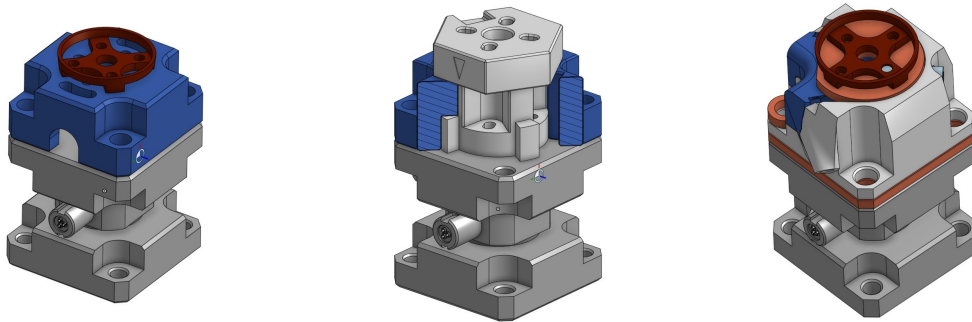


Figure 4.3: Different versions of the motor mount

substantially reduced the dead time between two tests.

Together with the motor mount, I also developed different sets of fairings in order to shield the load sensor from the flow and avoid measuring parasite drag. For this I simply used a symmetric NACA profile, adapting its size to avoid touching the inner components. For the second round of tests this was partially replaced by a poly-carbonate cover, that allowed to see the inside and act on failures rapidly.

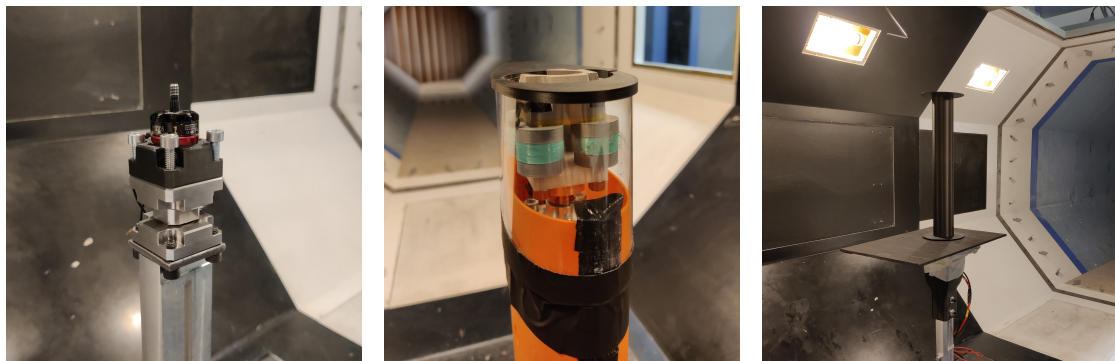


Figure 4.4: The test bench with the two versions and the slab

The fairings were mounted on both sides of the cylinder to make the setup symmetric and reproduce a similar setup as Badalamenti [3] and Price [7]. We then removed the top part that is not structurally essential. For the last part I designed a set of mounts that would allow to install a slab to simulate the interaction with the body of the craft.

4.3 Handling of the vibrations

A spinning body at high speed produces a lot of vibrations. This was encountered throughout the whole internship and was the biggest barrier to obtain good measures from the setup. The first round of test was characterized by an extremely high level of vibrations, with amplitudes in the order of tens of times the measured values of lift. This was greatly reduced by the redesign described in the previous section and the improvement of the printing techniques, but it was still not sufficient.

For this, after the first campaign, I dedicated several weeks to find suitable dampers to reduce vibrations. I first started by acquiring readily-available rubber dampers that proved to be not suitable: they would dampen some frequencies but amplify others.

I then decided to try printing dampers from a flexible material: for this we had to develop a technique and test configurations that would determine if the damper was appropriate. The testing protocol is fully described in appendix A.

The end results are the dampers that are showed in figure 4.4. These dampers are printed using a multi-material technique that consists in top and bottom PLA disks with threaded holes that allow to be screwed in directly and a sandwiched TPU layer. This layer is not solid and its filling pattern and density greatly impacts the dampening performances, as shown in the appendix A

The use of dampers does not solve completely the issue with vibrations, but greatly reduces its impact. We still need to extensively treat the data as shown in section 4.5.

4.4 Data acquisition

After discussing the mechanical setup of the test bench, this section will be about the electronic and numerical part.

4.4.1 Load sensors and measuring chain

During the internship the company had his offices at the Gipsa Lab in Grenoble, a research laboratory mainly focused on automatics and control. Thanks to the Gipsa Lab and M. Jonathan Dumon, a research engineer of the Gipsa, the company had access to two different tri-axial load sensors (figure 4.4) that have very different technical specifications. The first one, used in July, is a Kistler 9327C meant for loads up to $10kN$ and the second is a Kistler 9017 rated for $1kN$.

The definition of the load sensor was a tricky task, since we did not really have a choice and the amplifiers at the Gipsa Lab were not calibrated and did not work well with our setup. We realized that the Kistler 9327C sensor was not the most adapted during the first round of tests. With a sensibility of just $7pC/N$, it was indeed not suitable to precisely measure the light loads generated by the cylinders.

For the tests in October, we managed to have a new more adapted load sensor, with almost four times the sensitivity of the first one. This sensor, a Kistler 9017 was of a much smaller size and had to be adapted to the old setup via 3d printed parts.

During the initial phase of the internship I had grossly underestimated the difficulties related to the measuring chain. After the first problems with the amplifiers and the measurements, we realized that none of the equipment of the Gipsa had been properly kept and re-calibrated following the technical specifications of the manufacturer.

We observed that the majority of the issues were with the amplifiers: changing amplifier or even channel created major differences on the behavior of the drift and the measurement itself. We had to accept that acquisitions at Gipsa were not reliable.

Luckily, the ENSMA gave us the possibility to use their amplifier that is properly maintained and more precise thus allowing to exclude this uncertainty from the measuring chain. At the same time, the sensor used was also not fully calibrated and we have no way at the moment to estimate the presence or the magnitude of uncertainties lying with the load sensors itself. We tried measuring the weight known masses on different axis with good results and we concluded that the errors, when present, were negligible. As a final test, the obtained data had a reasonable order of magnitude.

4.4.2 Analog reading and saving

Raw data is acquired at 5 kHz through an analog-digital converter and delivered by the wind tunnel system in the form of a text file containing :

1. Time stamp;
2. Dynamic pressure;
3. Air density;
4. Air temperature;
5. Wind tunnel speed;
6. Measured force on x axis;
7. Measured force on y axis;
8. Measured force on z axis.

The Z axis was measured in a series of tests but was dropped due to the very disturbed nature of the signal, with non-linear drifts and too much cross-talk towards the other axis.

Fields 2 to 5 are directly recorded from or derived from the wind tunnel setup and they show good precision. Fields 5 to 8 are the result of the amplification

of the signals from the load cell. Measured forces present very high noise and disturbance, sometimes greater than thirty times the expected value and thus requiring accurate and extensive data extraction and noise reduction.

At the beginning of the test campaign the first objective was to determine if, despite the vibrations, some useful information was still encoded and easily retrievable. This was achieved by simply averaging the data in the intervals of constant rotational speed. I could easily find values that were coherent with the expected aerodynamics coefficients. This allowed for the prosecution of the tests.

Despite the availability of the measures, the presence of such high disturbances did not allow to decrease the measuring range of the amplifier thus reducing the overall precision. In fact, as stated before, the vibrations were sometimes even thirty times the aerodynamic force and the range of the amplifier was calibrated to avoid saturation having thus reducing the precision on the force itself.

Due to the vibrations and the lower precision, I was forced to only consider static behavior and exclude any dynamic effect or consideration based on the data.

4.5 Data treatment

Due to the assumption of only considering static phenomena, the entirety of the data treatment process revolves around canceling noise and finding the mean values in every region where lift and drag are constant due to α being constant. These regions can be identified as regions in the lift and drag curves where the values are constant: we called these regions "plateaux" (an example in figure 4.6).

Since the Arduino that controls the rotational speed of the cylinders does not provide with a time reference nor allows for precise constant time intervals for each value of α , the plateaux need to be automatically located and extracted starting from the measured forces.

The data treatment protocol, that will be later described in details, consists of the following phases:

1. General noise reduction;
2. Find the plateaux in the signal;
3. Calculate the rotational speed of the cylinder for every interval;
4. Import geometry and calculate the aerodynamic forces and coefficients;
5. Plot and save data;

In the following subsections I will describe in detail the first three points.

4.5.1 General noise reduction

The first step to obtain the plateaux is to reduce the noise: for this phase I'm not interested in determining the nature of the noise nor the exact value of the average

of the measures. An aggressive yet very effective filtering was used through a combination of Savitzky-Golay filters [21] [22]. The result is possibly not accurate since no distinction is made on the actual noise removed, but the obtained values will be used only to find the constant sections, while still providing a clear view of the static values of lift and drag.

To obtain more precised values, we calculate the module of the sum of the forces $F_e = \sqrt{F_x^2 + F_y^2}$ and we utilize this value to find the plateaux.

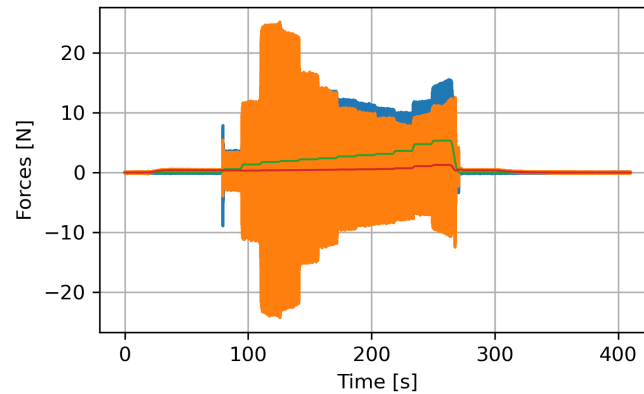


Figure 4.5: Effects of the Savitzky-Golay filter. We can appreciate the difference between the unfiltered lift (blue) and drag (orange) and the filtered data, lift (green) and drag (red).

Even if the treatment is aggressive, due to the nature of the data and the assumption on its use after the treatment, I assume that the vast majority of relevant data is preserved.

During data treatment we remarked that the length of every plateau is sufficient to obtain static values with sufficient precision. In fact, after a couple of seconds the mean converges to the measure.

Furthermore, the length of the steps together with the high frequency sampling allows as well for high precision in the spectral analysis to extract the rotational speed of the cylinder, as described later.

4.5.2 Detection of plateaux time segments for lift and drag calculation

In order to reduce to a minimum the impact of the filtering process, the previously obtained data is used to find the plateaux thanks to a simple algorithm.

With the aim of obtained synchronized values between lift and drag, the plateaux are calculated using the previously defined sum the sum of the forces, F_e . Once the plateaux are found on this force, the found time segments are then transferred to the lift and drag values. Due to the simple nature of the algorithm, the found

regions are trimmed on the sides to avoid in any circumstance the transitions and only use static values.

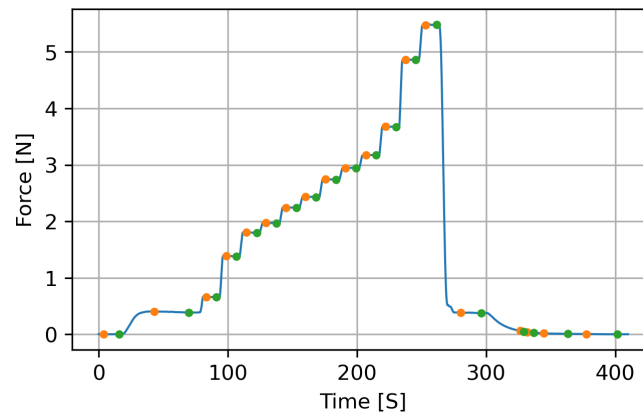


Figure 4.6: F_e filtered with the found start and end point for the plateaux, in orange and green respectively

Once the plateaux are found, the code uses the found time segments to compute a simple average on the raw data on both lift and drag and the calculated value is then stored and used to compute the aerodynamic coefficients. This step ensures that any possible error introduced by the filtering is not affecting the end results. This includes "smoothing" of the curve and any possible time shifts introduced by the filters. This ensures as well that any transitory phenomena is included in the final data.

During the development of this process, we tested the final values, obtained as in the previous paragraph against the equivalent average on the filtered curves of lift and drag, without founding noticeable differences. This can be used as proof that the assumptions on the treatment are valid and that our filtering can also be used to detect any weird behavior of the acquisition chain.

4.5.3 Extraction of rotational speeds and calculation of the aerodynamic coefficients

The Arduino used to control the motors can only send a PWM signal to the electronic speed controls (ESC) of the motors and nor the Arduino or the ESC have any closed loop control over the speed. This makes the imposed rotational speed not precised and thus requiring it to be calculated thanks to the spectrum of raw data. The high sampling frequency allows to obtain high precision. In any case, in order to provide a minimum frequency resolution, zero padding¹ is used to obtain the same

¹Zero padding, as explained by Orfanidis [21], is a technique that consists in adding zeros at the end of a time series before computing a Fourier transform. Since in general the number of

precision on all the data sets.

To calculate rotational speeds, the previously calculated time segments are used to extract raw data and perform a Fast Fourier Transform (FFT). In most cases the higher peak corresponds to the rotational frequency, but this is not always the case, and it was especially not the case without the dampers, where a lot of harmonics were present. For this reason, we still apply a focusing window around the expected frequencies and reject the others.

During the development of this method, the extracted frequencies were compared with the measured values with an optical tachometer and showed great accuracy. Since it was unpractical to use the tachometer in the tunnel, all data analysis was based solely on the spectral analysis. These can be also checked later once the velocity ratio is calculated to see if the calculated values are coherent.

At this point we have lift, drag and rotational speed for every time segments. Thanks to raw data, with a similar procedure used for lift and drag, speed and dynamic pressure are extracted and used to calculate α , C_L and C_D . This ensure that the correct set of data is used for each time segments and the coefficients are correct.

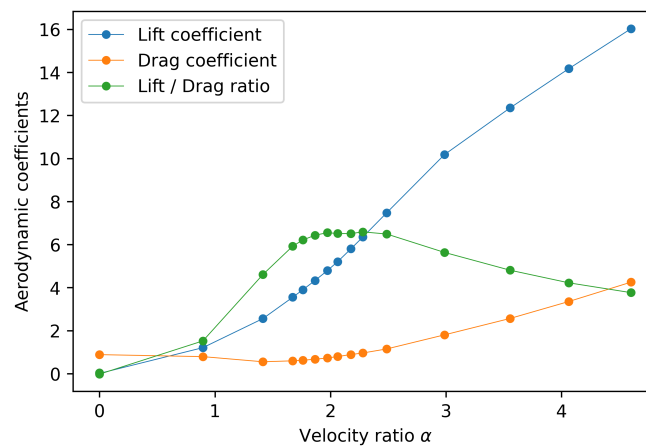


Figure 4.7: Calculated aerodynamic coefficients

frequencies at which we evaluate the Fourier's transform, adding zeros allows to increase the resolution in the frequency domain without altering the results

Chapter 5

Analysis of the results

After the first test campaign we realized that the data acquired, even after treatment, was unusable especially considering the measurement of the drag: even though some tests showed curves that were in line with the literature, we had no way to determine a degree of confidence and to establish which measures were acceptable and which were not. For these reasons all the results proposed here are obtained from the second round of tests.

During this second series of tests, we collected many more tests and we made sure to have plenty of similar configurations that would allow to determine the confidence in the measures. After carefully screening the data, we had to drop some tests that showed acquisition errors, sometimes ending with results completely incoherent with the laws of physics.

5.1 Procedure to utilize data

In this section I will explain what criteria were used to determine if a test was acceptable and how we determined if the overall measures were usable to extrapolate trends. I will also discuss how data is later presented in the analysis.

5.1.1 Repeatability

The first and foremost method is the repetition of similar tests many times. For this, we made sure to change the physical cylinder and perform full disassembly and reassembly together with simply redoing the acquisition.

We were able to see that running the same test without disassembly gave mostly the same results, as shown in picture 5.1, proving that the chain of measure was not adding a lot of noise and overall the setup was acceptable. We then repeated some tests after disassembly: we observed more dispersion than in the previous case, but still in a reasonable range, as can be seen in figure 5.2.

Unfortunately, the level of vibrations is dependent on the assembly and even a small difference can change significantly the amplitude of the vibrations. We were

able nevertheless to address this issue and pay attention to the assembly of the cylinder and we did not encounter many differences in the tests.

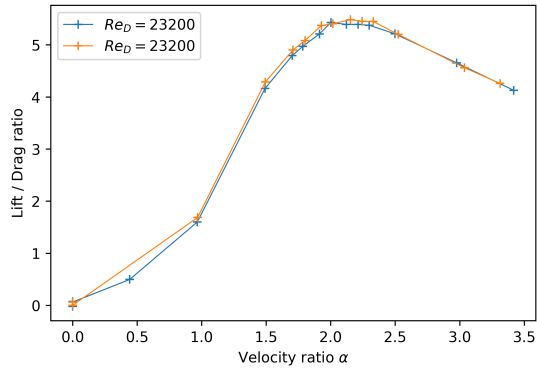


Figure 5.1: Test of repeatability without disassembly ($D = 35mm$, $\Lambda = 5.1$, $R = 2$, symmetrical)

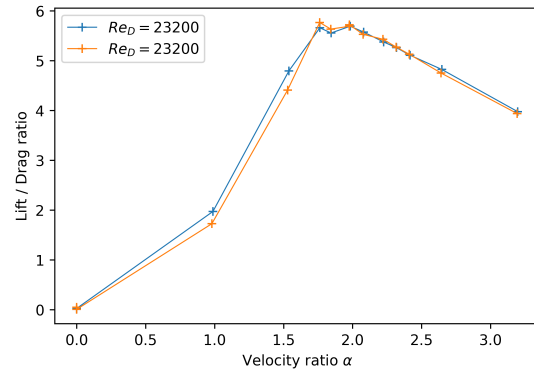


Figure 5.2: Test of repeatability with disassembly ($D = 35mm$, $\Lambda = 6.5$, $R = 2.9$, asymmetrical)

5.1.2 Effect of Reynolds number (Re_D)

The tests were conducted at different speeds ranging from $5m/s$ to $15m/s$ and with cylinders of two different sizes in order to understand the dependency between the coefficients and the Re_D . As exposed previously, the literature clearly shows a variation with the Reynolds number, but this occurs with a wider range of values of Re_D .

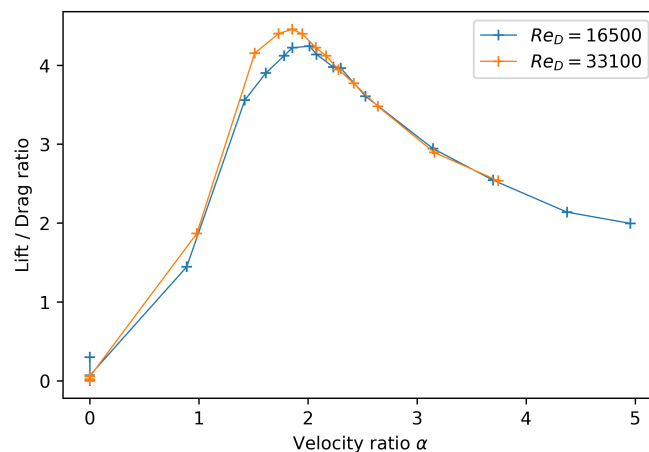


Figure 5.3: Test of influence of Reynolds number on the efficiency

During our tests we adopted cylinders with a diameter of 35mm and 50mm , that gives Reynolds number (Re_D) ranging from 12500 to 35500. In the tests, we were limited by the rotation speed of the motors and consequently by the induced vibrations. Also, the chosen range of Re_D was the most relevant for the short-term interests of the company.

As shown in figure 5.3, we can see that the differences seen in the data points are coherent with a dispersion of 5%, as described in the following subsection. We accepted, after verifying other sets, that no significant dependency of Reynolds number was observed, at least for α lower then the lift plateau . It is also important to note that being able to reduce the speed of the flow allows for lower vibrations and overall cleaner results.

5.1.3 Presentation of the data

After verifying the quality of the data we remarked that all the accepted sets showed, especially for the efficiency, a deviation of not more than 5% from the interpolated curve, as shown in figure 5.4. This chosen deviation, even if probably not perfect, is more than sufficient to present trends in the data: we estimated that differences below 5% were not relevant as results for this work as the setup does not allow for such small resolution. It is to be noted that the objective of this presentation is to give and study trends, not actual punctual values.

Similarly to the experience of Badalamenti and Prince [3], where no distinction was made based on speed, I opted to present the results neglecting the influence of Reynolds number. This assumption is based on the previously presented data.

From the following section, diameter and speed will be neglected and only one curve will be presented per set of parameters, even if more are available.

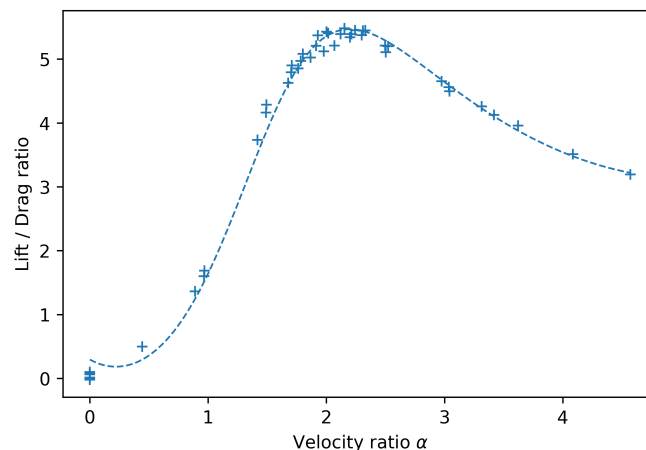


Figure 5.4: Typical dispersion on one configuration ($D = 35\text{mm}$, $\Lambda = 6.5$, $R = 2.9$, asymmetrical, various Re_D)

5.2 Effect of the aspect ratio (Λ)

As mentioned in the objectives of the internship, the aspect ratio is probably the parameter on which there was the least amount of clear information from the literature. After discarding bad data, we were left with a few sets that show its influence without modifying any other parameter.

As we can see in figure 5.5 we observe almost no influence on the lift coefficient of the aspect ratio on values of α lower than 3.5. After this value we can remark that the tests with the lowest aspect ratio start to encounter the plateau that is well documented in the literature. For higher Λ , the plateau should come at higher speeds and it was not reached in our tests.

We can also note that in the range of velocity ratio from 1 to 3.5, all the curves have a clear linear trend that does not depend on the Reynolds number. We do not have sufficient data to give pertinent trends at α lower than 1.

The overall behavior of the lift coefficient is coherent with the literature and resembles what found in Badalamenti [3] and reported in figure 2.7.

Regarding the trends with the drag coefficient, we can see that all of the tests show a common intersection point in the range of α from 1.5 to 2.5. Before this point, seemingly depending on the other parameters, lower Λ amounts to lower drag. After this point the opposite occurs: with higher Λ the drag decreases substantially. Figure 5.6 clearly shows this trend and the inversion.

We are unsure of the nature of this inversion and it is not documented in the literature. We consider that it might be due to more bending of the test setup or general issues in the measures. On the other hand we do not exclude that it might be a physical phenomenon that we need to further investigate. It is true that this is shown on most of our curves, but it's particularly evident with higher aspect ratio and with the disks, as shown later in 5.3 and it definitely needs further testings.

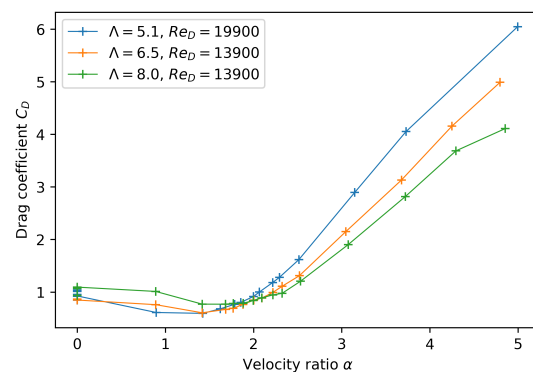
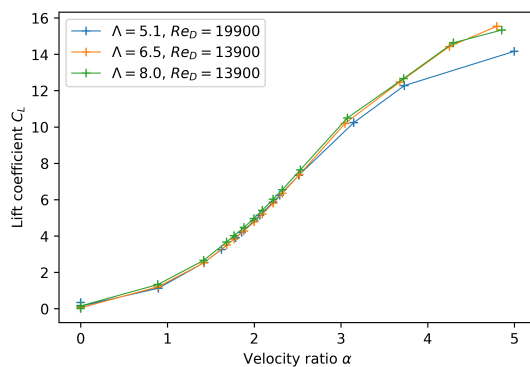


Figure 5.5: Influence of Λ on C_L ($R = 2$, symmetrical) **Figure 5.6:** Influence of Λ on C_D ($R = 2$, symmetrical)

Regarding the influence of the aspect ratio on the efficiency, we can see that

overall higher Λ gives higher values. The position of the peak also varies, moving towards higher values of velocity ratio (α) with higher aspect ratio. This is represented in figure 5.7

As expected from the literature, the peaks are located in a range of α from 1.5 up to 3 with the highest elongations. As per the values of drag, we can remark an inversion in the region before the peak: lower Λ gives slightly higher efficiency due to the lower drag. Figure 5.7 shows this trend.

Overall, the trends that I extracted from our data are quite in line with the literature and common knowledge. This behavior is in fact similar to that of a standard wing. These trends can now help the design phase according to the required performances or the structural needs of the company.

Trying to properly quantify the impact for a real optimization is however quite difficult considering the limited samples. I estimated that, at least up to an aspect ratio of 8, for every unit of Λ , the peak of efficiency is increased by around 10%, moving a little depending on the configuration.

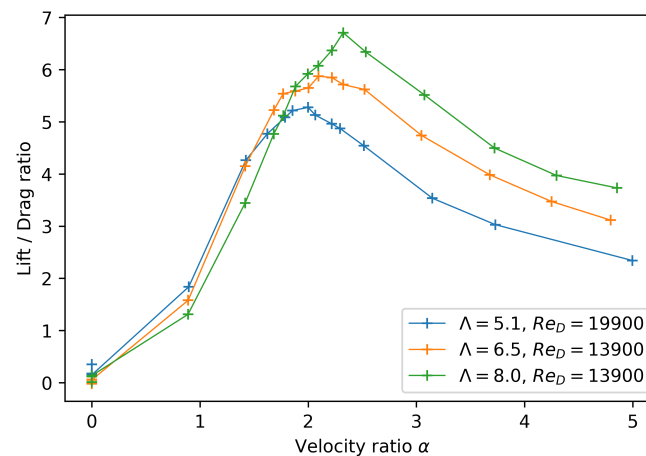


Figure 5.7: Influence of Λ on the efficiency ($R = 2$, symmetrical)

5.3 Effect of end plate ratio (R)

We could observe that varying the size of the disks has a similar effect as the variation of aspect ratio: the lift curve, visible in figure 5.8, always shows a linear phase up to $\alpha = 3.5$ and then decreases if R is reduced, up to the point of seeing the plateau with small R and Λ . Smaller disks or shorter cylinders should show a plateau, but we were not able to reach the needed values of α and we had to drop some of the tests due to bad data.

The effect on drag, in figure 5.9, follows again the same trend as the aspect ratio. We see the same inversion that was observed in figure 5.6: bigger disks have higher drag at lower velocity ratio and lower drag at higher α and vice versa.

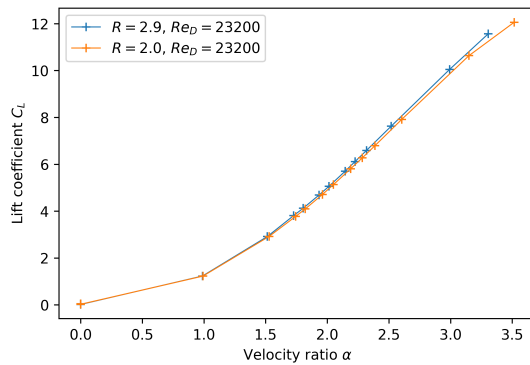


Figure 5.8: Influence of R on C_L ($D = 35\text{mm}$, $\Lambda = 6.5$, symmetrical)

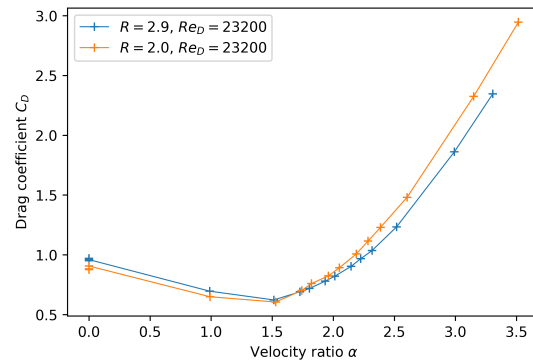


Figure 5.9: Influence of R on C_D ($D = 35\text{mm}$, $\Lambda = 6.5$, symmetrical)

As expected from the curves of lift and drag, in case of a modification of R the efficiency acts similarly to a modification of Λ . With bigger disks the maximum is higher and moved towards higher velocity ratio, as can be seen in figure 5.10.

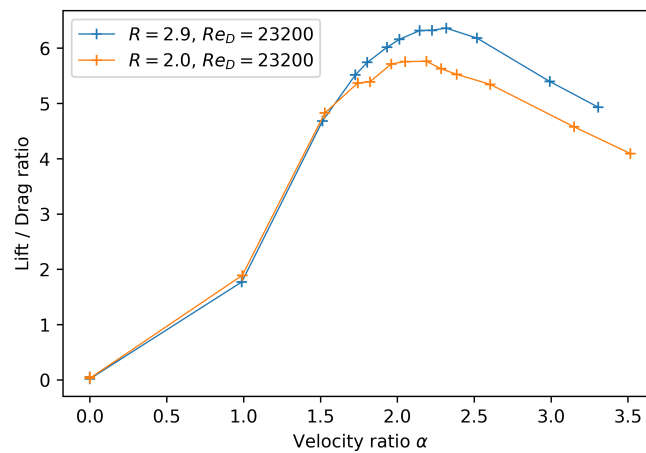


Figure 5.10: Influence of R on the efficiency ($D = 35\text{mm}$, $\Lambda = 6.5$, symmetrical)

If we want to try and quantify the effect of these variables, we can estimate that one unit of R is the equivalent of around 1.5 units of aspect ratio, at least for shorter cylinders.

It is important to note that during all the tests the measured forces are those of the coupled cylinders and disks, as it was not possible to simply measure the forces on the cylinders alone. It could be interesting to decouple in the future the two elements to better understand the impact on the global performances.

5.4 Effects of the asymmetry

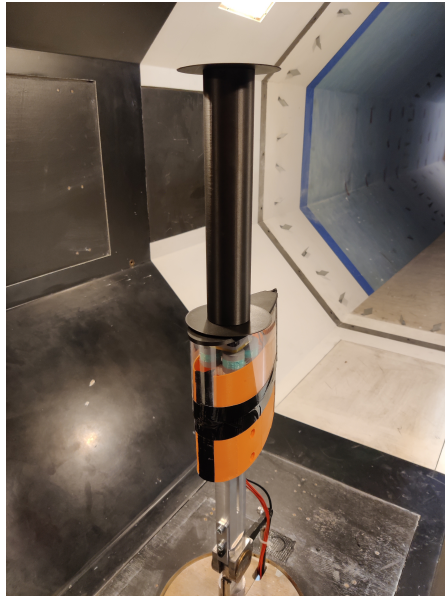


Figure 5.11: The experimental setup for this configuration

The absence of the top fairing introduces effects at the end of the wing that reduce its performance. The resulting effect is similar to that of a lower aspect ratio. We can see in the data that without fairing we encounter sooner the plateau, but the linear region is left untouched.

While the lift coefficient, shown in figure 5.12, follows common patterns, the drag curve, shown in figure 5.13, does not show an inversion, differently from the aspect ratio. We observe that removing the fairing simply increases drag for the whole range of velocity ratio. We can see that the increment is neither constant nor proportional to the magnitude, as at lower α it is around 20% and at higher speed it decreases.

With the asymmetry, the efficiency, shown in figure 5.14, is lowered when the fairing is removed and the peaks are not significantly moved.

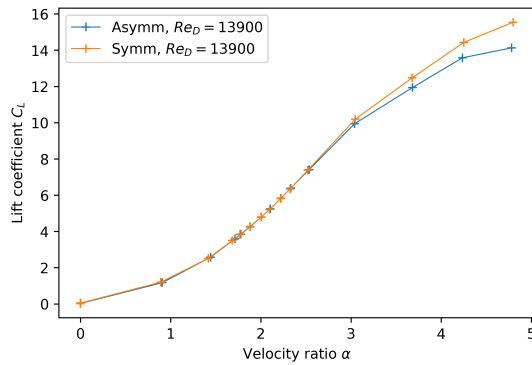


Figure 5.12: Influence of the asymmetry on C_L ($D = 35\text{mm}$, $\Lambda = 6.5$, $R = 2$)

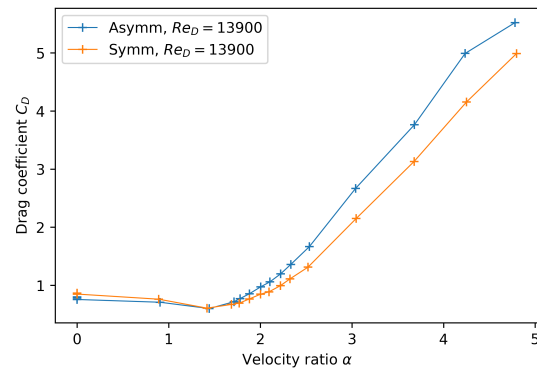


Figure 5.13: Influence of the asymmetry on C_D ($D = 35\text{mm}$, $\Lambda = 6.5$, $R = 2$)

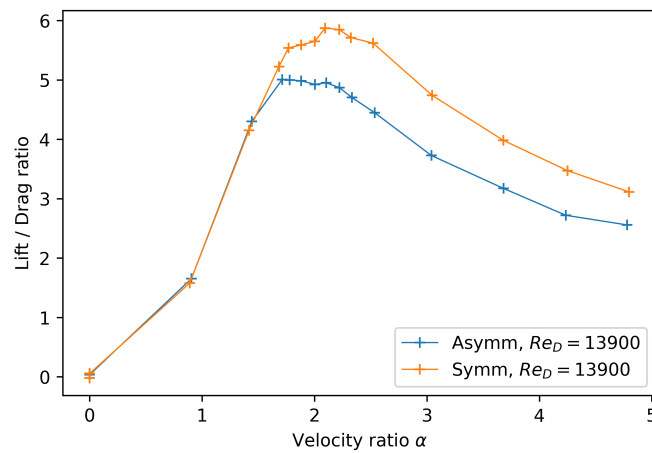


Figure 5.14: Influence of the asymmetry on the efficiency ($D = 35\text{mm}$, $\Lambda = 6.5$, $R = 2$)

Here, we can estimate that the asymmetry generate a loss in efficiency of around 10 to 15%, once again dependent on the geometry.

5.5 Effect of the plaque

This set of tests is quite interesting as it considers environmental conditions for the wings. We opted to use a slab that allows to introduce a mixture of boundary layers, pressure gradients and a strong asymmetry in general. We were not focused for this experiment on the simulation of a specific condition.

It is important to note that we do not have many repetitions for this tests and a lot of the interest of this part was to develop a proof of concept of such a test.

Nevertheless, we were able to extract enough data to start a first reflection on the matter. For this we compared six different configurations of end disks with the same cylinder and the same speed.

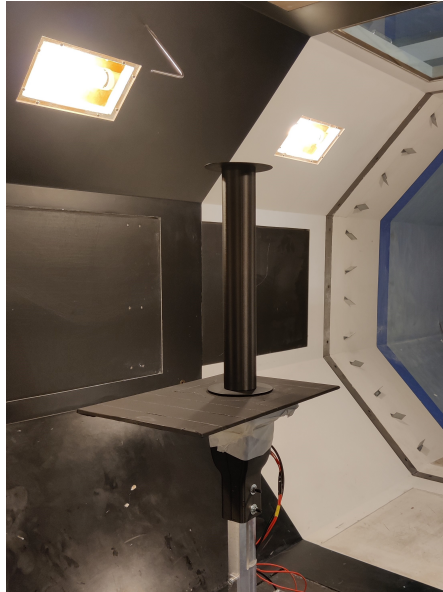


Figure 5.15: Experimental setup for this configuration

Regarding the test conditions and the type and size of the boundary layer, we were essentially forced by the material we could find and by mechanical constraints. The speed of the wind tunnel was set at $6m/s$ to reduce vibrations and flexion and the size of the plaque was imposed by the availability of scraps at Gipsa. While for the other tests the importance of speed can be neglected, for this one speed was kept as constant as possible in order to obtain more consistent conditions of boundary layer.

This test condition does not reproduce in any way an existing situation on any drone, but it is a start to understand a more academic condition that can be reproduced later without particular difficulty.

The first two configurations were classical cylinders with disks of $R = 2$ and $R = 2.857$. We could see an overall decrease of performance comparing with the same tests in the asymmetrical configuration, especially in the form of an increase of drag and thus an overall reduction of efficiency. The magnitude of this reduction appears to be similar to that of passing from our symmetrical to asymmetrical cases, but due to the lack of data it is difficult to properly quantify this value.

In any case, I could not observe any particular trend that seemed incoherent with the rest: bigger disks still produce higher efficiency and the increase in efficiency increasing the disks is coherent with what was previously presented, even if slightly lower.

We later tested asymmetrical configurations: these configurations are called

following the table 5.1. This series was to see if the lower disk, the one close to the plaque, was as important as the top disk in determining performances

| Conf | Bottom disk | Top disk |
|------|-------------|----------|
| 2 | 2 | 2 |
| 3 | 2.857 | 2.857 |
| 5 | 2 | 2.857 |
| 6 | 2.857 | 2 |
| 7 | 1.05 | 2 |
| 8 | 1.05 | 2.857 |

Table 5.1: Naming of the tests in the boundary layer

Starting from configurations 5 and 6, we could see that the impact of the top disk seems to be more important than the other: not only the two curves are not equal, they are very different with more drag (figure 5.17) in the case of the smallest disk on top. Comparing the efficiency in figure 5.18 we can see that the difference is quite noticeable. Moreover, it is very interesting to note that the curve of configuration 5 is very similar to the symmetrical configuration with two big disks, as if the bottom disk was not very influential.

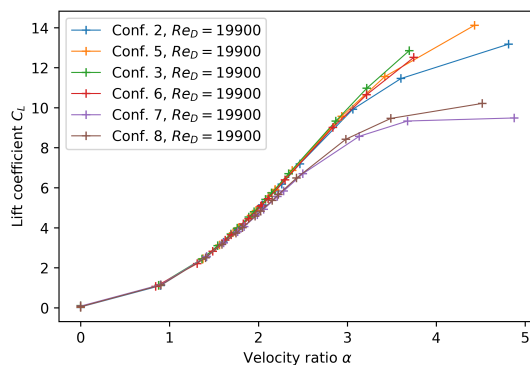


Figure 5.16: Influence of plate on C_L ($D = 50mm$, $\Lambda = 6.5$)

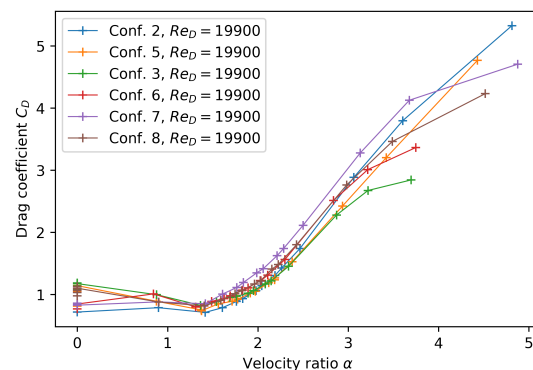


Figure 5.17: Influence of plate on C_D ($D = 50mm$, $\Lambda = 6.5$)

In order to verify this hypothesis, tests with configurations 7 and 8 were conducted, with almost no disk at the base and different disks on top. We could see for the first time, as shown in figure 5.16, a substantial degradation of the lift coefficient at low α : we clearly obtained the plateau at speeds starting from $\alpha = 2.5$. It is interesting to note that the two curves of lift are anyway similar.

Checking the drag coefficient in figure 5.17, we observed that, as expected, bigger disks give lower drag and once again we were able to see the inversion

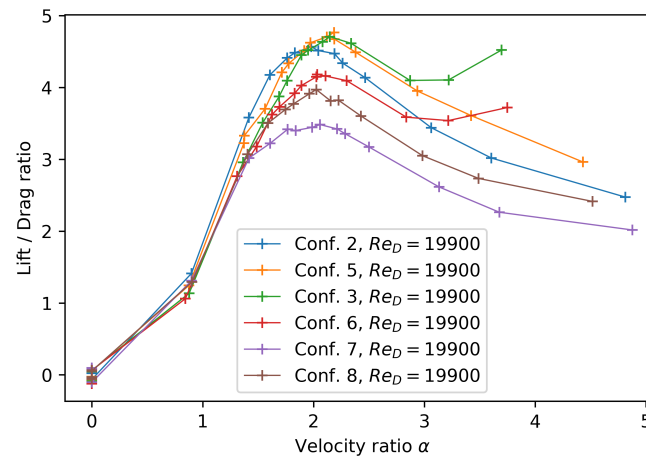


Figure 5.18: Influence of plate on the efficiency ($D = 50\text{mm}$, $\Lambda = 6.5$)

phenomenon. Finally, we observed that the efficiency, as in figure 5.18, was significantly lower than any of the other tests: the least efficient case was configuration 7, with the small disk at the top. While this is clear and expected, we clearly registered that completely removing the disks, even in a boundary layer, really affects the performances.

I found very interesting the trend where a slightly smaller disk at the base did not create a proportional difference in this boundary layer condition (see configurations 3 and 5). This information could be extremely beneficial for the company as most of the times the size of the disk closer to the drone is limited by the available space on the chassis.

Of course, the data we acquired, even if interesting for a first try, is very incomplete and needs to be reproduced again in different conditions. Also, we do not dispose of asymmetrical tests without boundary layer or in the symmetrical configuration, which could shed a more complete light on our findings.

Chapter 6

Perspectives and critical points

This project helped clear the path towards a better development of the Chronics products. It helped highlight some difficulties that were not anticipated at the beginning and gave valuable information on how to improve research in this field.

6.1 Mechanics and setup

Before discussing the aerodynamics, I would like to discuss a few elements that emerged during the internship and that are, in my opinion, essential for the improvement of the quality of future work.

6.1.1 Design and vibrations

The first point I would like to discuss is mechanics. Even if my internship was based on the aerodynamics of Magnus effect wings, a lot of work was done in order to achieve the results. The most important issue, as mentioned, is vibrations.

Even though we managed to control vibrations during the wind tunnel tests, the use of dampers will probably not be possible in flight for the added mass and complexity it would imply. This work showed that these wings are quite complex systems due to the very high rotational speed and the design greatly impacts the handling of vibrations.

During the internship I redesigned the cylinders twice with substantial improvements at each iteration. Nevertheless, the final design is probably not fully adapted for flight conditions as it is not mass-optimized. I believe that Chronics should do further work towards the reduction of vibrations with more optimized designs, better motors and a better understanding of the influence of other variables, such as mountings, materials, etc. on the overall system.

6.1.2 Manufacturing and 3D printing

I would like to discuss as well on the manufacturing processes that were utilized and improved during the internship and in general at the company.

As mentioned, the vast majority of parts, being them cylinders, mounts or anything else, is 3D printed in-house. For this we have been trying different materials and different techniques. 3D printing is a very powerful tool and, without it, it would have been nearly impossible to achieve the results presented in this work.

Anyhow, the extensive use of the technology highlighted that we need to further develop techniques to ensure consistency between different printers, as well as to make sure that the errors introduced by printing do not affect considerably the final product, especially on the vibrations.

Another interesting topic of research could be the use of more advanced materials: better understanding each available material and its potential uses could help reduce mass and improve the mechanics of the overall product.

A detailed analysis on the printing technique should be conducted for each materials, preparing a test protocol to evaluate the performances of the material and the material in relation to the printing technique.

6.1.3 Measuring chain

One aspect that was very difficult to handle was the acquisition of the aerodynamic values, both in the wind tunnel and at Gipsa. Even though we managed to obtain quality measures during the second round of tests, I believe that a thorough research should be conducted on how to properly measure the forces of this kinds of wings.

It would be interesting in fact, for the continuation of this research, to be able to increase the precision in order to study smaller variations and have more confidence in the actual values instead of the trends.

During some tests we tried to measure the third component from the sensor but failed: the measured data showed a behavior that we were unable to understand. It showed very high and non-linear drift that, when partly corrected, did not reveal the plateaux. We suspect that there issues could be caused by the vibrations or by an incorrect pretension of the load sensor. An example can be seen in figure 6.1.

For the following tests it could be interesting to develop such a system that would allow for force measuring on both ends of the cylinder: this would allow for more stable measures and also would prevent the bending discussed in section 6.2.1. In any case, extensive calibration and verification of sensors and amplifiers is absolutely necessary for any further test.

6.2 Aerodynamics

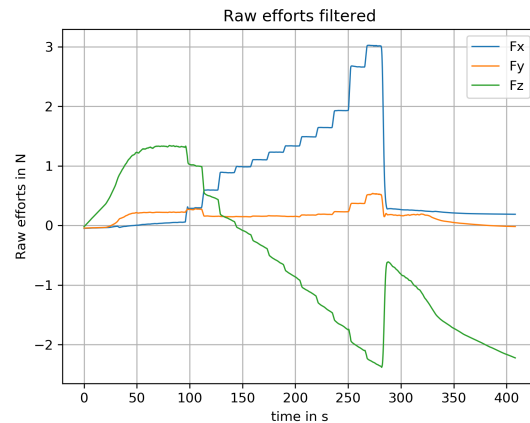


Figure 6.1: Visualization of the z component

6.2.1 Anomalies and difficulties

At the end of the tests we were glad to find many curves that were coherent with the expected physics and the literature. Nevertheless, we encountered many cases where some anomalies were clearly visible.

In some tests the values of the measured drag were quite low, so low that the calculated efficiency was more than 50. Up to this moment I have presented all the results in terms of coefficients, but I have to remind that such a variation of efficiency can be caused by a variation of as little as $0.1N$. Measuring drag was an especially hard challenge considering that the amplitude of the vibrations was around $40N$.

We suspect that this issue is related to the quality of the measures that on the drag component is especially lacking. All the tests with incoherent values of efficiency were dropped due to lack of other similar tests or discrepancy between similar tests.

In some other cases we noted a difference with the diameter: we saw, for very similar Reynolds number, lower values of efficiency in the case of larger diameter. We suppose that one reason of this could be the flexion of the cylinders on the base: the dampers seem not to provide sufficient rigidity for these tests. While we assumed that the aerodynamic coefficients, as a first approximation, do not depend on Re_D , the raw values of the aerodynamic forces increase with the diameter and speed, thus increasing the bending.

After observing these anomalies we conducted a test by taking pictures of the cylinders in different conditions of the cylinder and noted in fact a non negligible flexion. We paid attention to conduct the analysis of results without proposing comparisons with different diameters when possible in order to mitigate the effect of this. An example of this anomaly is available in picture 6.2.

Some other tests simply presented data too scattered to be used without

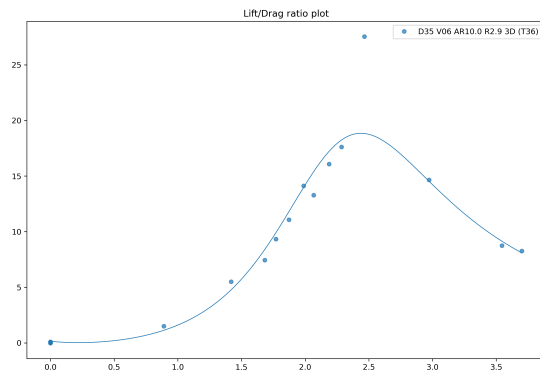


Figure 6.2: An example of non-physical efficiency

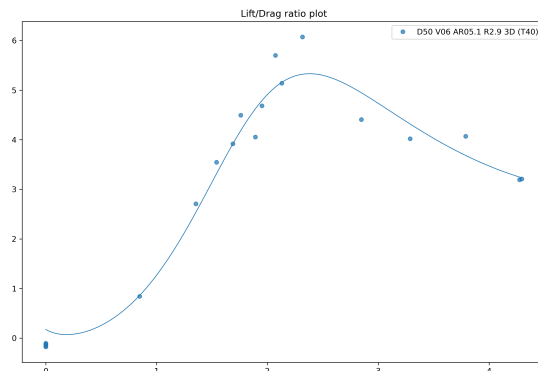


Figure 6.3: An example of excessive scatter

accepting a too low level of precision. These tests were consequentially dropped, similarly to the test in picture 6.3.

6.2.2 Future development

This work was limited by many factors, especially the need to develop the test bench and the test protocol. We are overall satisfied by the different results obtained but clearly more can be done to understand and master the Magnus Effect.

The internship was meant as the introduction to a doctorate to be conducted on the same subject. In this part I will try to articulate possible ideas that could be investigated during such PhD.

Asymmetrical and different disks configurations

As done in the case of the boundary layer tests, one path that could be interesting is the asymmetrical configuration. The study of the effects on different size of disks has been briefly studied by Badalamenti [**badalamenti**], but can be further investigated especially with the idea of installing such wings on crafts where geometrical limitations are impossible to avoid.

Furthermore, starting with asymmetrical configurations could allow for much bigger disks at the open side (for 3D configurations), disks that would be impossible to install symmetrically on a craft. Such configurations are, to my knowledge, not available in the literature.

High aspect ratio and variation prediction

First of all, we were unable to properly measure the performances of high aspect ratio, due to the different problems already described. It would be very interesting

to test even higher values to try and reproduce as much as possible the ideal bidimensional configuration.

If our hypothesis on the source of our issues is correct, improving the test setup and the acquisition chain should allow for this kind of tests. Improving the tests conditions would allow as well to pass from measuring trends to measuring values.

Measuring and increase the precision of the values would also allow to properly measure the trends in the phenomena and their impact. Especially for the purposes of the company, being able to estimate beforehand the behavior of a specific wing could be extremely valuable.

Surface finish and geometry

Another important aspect that we were not able to consider is the surface, as for this internship we did not dispose of a way to reproduce the roughness in a controlled manner. It is important to note that, even if the roughness was unknown, we were able to maintain the same surface finish thanks to the manufacturing process. We know from the literature that the surface finish is extremely relevant in the definition of the drag and, while, some studies have been conducted already in that direction, more can be done to extract prediction models and to be able to reproduce certain textures with 3D printing.

While some publications are available on surface roughness, not many are available on the actual geometry of the cylinders. Some tests have been conducted on the use of ribs or diamonds on the surface, but a lot more can be done with more complex geometry. Thanks to the company's expertise with 3D printing, creating new and more complex geometries should be quite easy.

Finally, tests can be made in order to test even more complex 3D geometries such as conical cylinders or bi-conical shapes. More shapes can be considered in order to fit on specific applications or with specific mechanical needs.

Measurement of power consumption

Even though we were already able to measure the power consumption of the spinning motor, this was not done during this internship because the cylinders we tested are very different from the flight configuration, especially in terms of mass.

Studying the effect of the different parameters, especially the surface texture and geometry on the power consumption could be extremely interesting to evaluate the energy balance of the complete system.

Interactions with other flows

The first tests conducted with the boundary layer showed that the differences are not negligible, much more should be done to understand the effect of such interference starting with other plaque configurations with different boundary layer conditions. Another idea could be to actually attach the wing to the body of a drone and try to reproduce the effect in flight.

Furthermore, the interaction of bodies in different position relative to the wing could be studied: this can be for example the arm of the drone's motor. Also, the effect of a motor blowing on different parts of the wing should be studied.

It is clear that these configurations are quite challenging and could depend very much on the installation, but I believe that this data could be of great interest for the development of a functional product and for the research itself.

Interaction with atmospheric wind and gusts

The tests conducted during this project were all in a wind tunnel with very low turbulence and no wind speed variations. It would be interesting to develop a series of tests in more real but controlled wind conditions with higher turbulence, gusts and cross winds. These tests can be conducted in specialized wind tunnels or by adapting the tests conditions accordingly.

For this it will also be interesting to test the system using an active control system for the speed similar to that of the final product.

CFD analysis

Finally, after having gathered more and more precised data, CFD analysis could be the following step in the Magnus Effect research.

As mentioned in section 1.2.2 many authors have studied and continue studying the Magnus effect in simulation. The results, even if interesting, do not answer for the time being the issue of calculating aerodynamic coefficients in unconventional cases for practical use. More experimental data could help the developing a functional model for our uses and would be beneficial both for the product and the research.

For the first, it would allow to test different configurations for a specific drone and adapt quickly and, on the long run, cheaply. For the latter it would allow to roughly test new configurations and then test in the wind tunnel the most interesting cases.

Chapter 7

Conclusion

Being in a small company allowed me to explore many different subjects and made me quickly learn different new skills. Surely I could learn a lot on the main subject which was the experimental study of wings.

I was able to understand the process behind the development of a test protocol, the setup and the exploitation of data, the resolutions of problems in the long and short term and I'm deeply grateful to everyone that took part in this journey.

Apart from this main focus, I was able to dive into the mechanics of high speed spinning devices, discovering new methods and techniques. I learned a lot on vibrations and their management, on dampers and on precision manufacturing. I was also able to learn techniques to treat data and filter disturbances and to control the test bench. Furthermore, I can now say to have a good knowledge of 3D printing, with its power and limitations.

Overall I think that this project was a very interesting conclusion to my engineering degree and really challenged me to real applications of many of the things that I was able to learn during these years.

Finally, on a more personal note, one major aspect of this internship is that in these six months I was able to really experience what research and development means and I will probably keep this forever with me. I discovered the thrill of exploring new things, but as well the fear and discomfort of navigating in the dark and even failing. I learned that sometimes it takes a lot of trial and error just to make one simple thing work, but also the satisfaction of seeing the results of my hard work. I believe this will be extremely valuable to me in the future as an engineer, especially with my intention to continue doing research.

Appendix A

Dampers test protocol

As mentioned in section 4.3, during the design of the dampers a test protocol was developed to evaluate the quality of our work. For this, we used a motor with an unbalanced mass attached to the shaft that would spin at increasing speeds. The whole setup was mounted to the load sensor.

Using the load sensor we acquired all the data and thanks to a portable oscilloscope we performed an FFT. The FFT is performed using data of a certain interval of time much longer than the recording frequency. The output graph is the representation of the peaks in all FFT: for each point the highest value of the test is taken. This allows to see overall the range of frequencies that behave best and worst.

The images acquired with this method show on the x-axis the frequency in Hertz and on the y-axis the peak expressed in volts. The amplifier was set to $10N/V$. We can clearly see an improvement in the proposed graphs

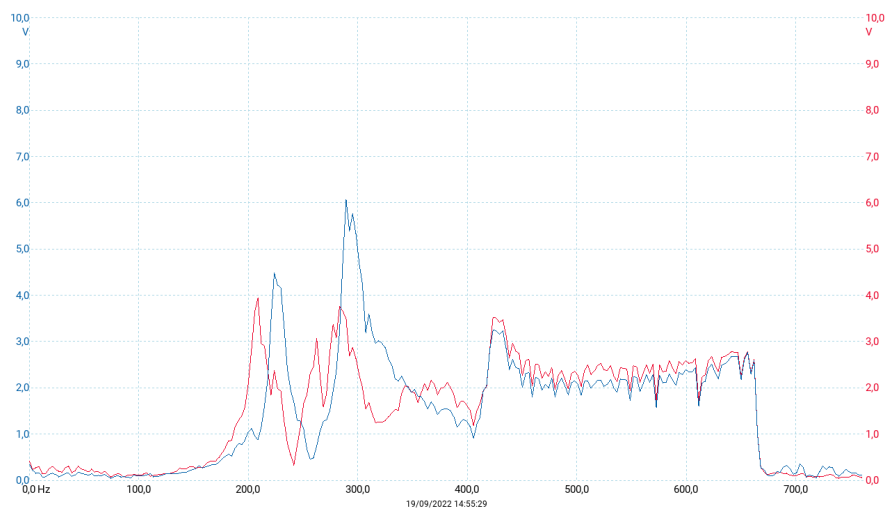


Figure A.1: The representation of the system without dampers

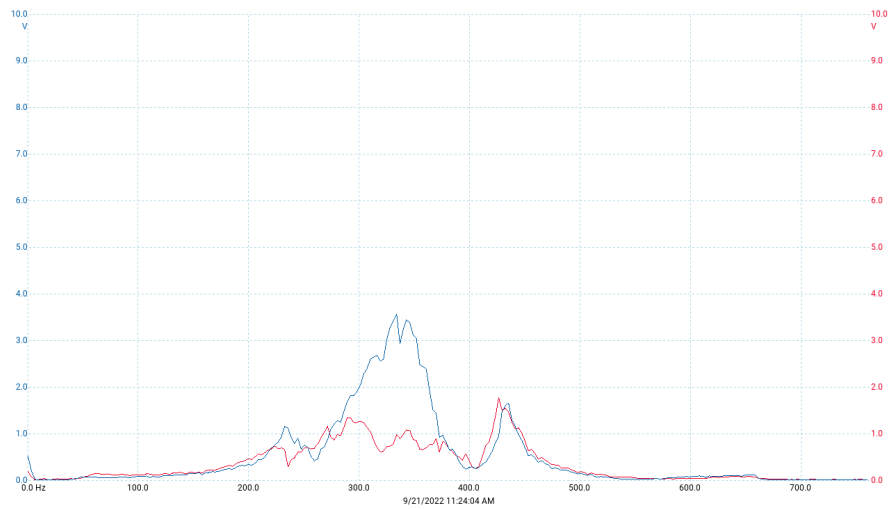


Figure A.2: The representation of the system with a set of dampers

Bibliography

- [1] W. M. Swanson. «The Magnus Effect: A Summary of Investigations to Date». In: *Journal of Basic Engineering* 83.3 (Sept. 1, 1961), pp. 461–470. doi: 10.1115/1.3659004.
- [2] H. M. Badr and S. C. R. Dennis. «Time-Dependent Viscous Flow Past an Impulsively Started Rotating and Translating Circular Cylinder». In: *Journal of Fluid Mechanics* 158 (Sept. 1985), pp. 447–488. doi: 10.1017/S0022112085002725.
- [3] Carmine Badalamenti and Simon Prince. «Effects of Endplates on a Rotating Cylinder in Crossflow». In: *26th AIAA Applied Aerodynamics Conference*. 26th AIAA Applied Aerodynamics Conference. Honolulu, Hawaii: American Institute of Aeronautics and Astronautics, Aug. 18, 2008. doi: 10.2514/6.2008-7063.
- [4] Nicolas Thouault, Christian Breitsamter, Nikolaus A. Adams, Jost Seifert, Carmine Badalamenti, and Simon A. Prince. «Numerical Analysis of a Rotating Cylinder with Spanwise Disks». In: *AIAA Journal* 50.2 (Feb. 2012), pp. 271–283. doi: 10.2514/1.J050856.
- [5] Alaa Elmiligui, Khaled Abdol-Hamid, Steven Massey, and S. Pao. «Numerical Study of Flow Past a Circular Cylinder Using RANS, Hybrid RANS/LES and PANS Formulations». In: *AIAA*. Sept. 2004. doi: 10.2514/6.2004-4959.
- [6] Wei Zhang, Rickard Bensow, Valery Chernoray, and Maxim Golubev. «Flow Past a Rotating Finite Length Cylinder: Numerical and Experimental Study». In: *51st AIAA Aerospace Sciences Meeting Including the New Horizons Forum and Aerospace Exposition*. 51st AIAA Aerospace Sciences Meeting Including the New Horizons Forum and Aerospace Exposition. Grapevine (Dallas/Ft. Worth Region), Texas: American Institute of Aeronautics and Astronautics, Jan. 7, 2013. doi: 10.2514/6.2013-987.
- [7] Prince, Simon, Holt, Jenny, and Episkopou, Petros. «Geometric Roughness Effects on the Aerodynamic Characteristics of a Spinning Cylinder in Cross-flow». In: *30th Congress of the International Council of the Aeronautical Sciences*. ICAS 2016. Daejeon, Korea, Sept. 2016.

- [8] Thom, A. *Experiments on the Flow Past a Rotating Cylinder*. (Air Ministry. Aeronautical Research Committee. Reports and Memoranda). Aeronautical Research Committee, Air Ministry, 1931.
- [9] Reid, Elliot G. «Tests of Rotating Cylinders». In: *NACA Technical Notes* 209 (Dec. 1924).
- [10] C. Badalamenti and Simon Prince. «Vortex Shedding from a Rotating Circular Cylinder at Moderate Sub-Critical Reynolds Numbers and High Velocity Ratio». In: *ICAS Secretariat - 26th Congress of International Council of the Aeronautical Sciences 2008, ICAS 2008* 6 (Jan. 2008), pp. 404–414.
- [11] Erwin Gowree and Simon Prince. «A Computational Study of the Aerodynamics of a Spinning Cylinder in a Crossflow of High Reynolds Number». In: 28th Congress of the International Council of the Aeronautical Sciences 2012, ICAS 2012. Vol. 2. Sept. 1, 2012.
- [12] Anderson Proença, Karl Gerhard, Simon Prince, Kevin Garry, and Theophile Tragin. «Roughness Effects on the Aerodynamic Forces and Wake Flowfield of Spinning Cylinders». In: June 27, 2022. doi: 10.2514/6.2022-4021.
- [13] Borg, John. *Magnus Effect: An Overview of Its Past and Future Practical Applications*. AD-A165 902. Departement of the Navy, USA, Mar. 1986.
- [14] G. Bordogna. «Aerodynamics of Wind-Assisted Ships: Interaction Effects on the Aerodynamic Performance of Multiple Wind-Propulsion Systems». In: (2020). doi: 10.4233/uuid:96eda9cd-3163-4c6b-9b9f-e9fa329df071.
- [15] Jost Seifert. «A Review of the Magnus Effect in Aeronautics». In: *Progress in Aerospace Sciences* 55 (Nov. 2012), pp. 17–45. doi: 10.1016/j.paerosci.2012.07.001.
- [16] V.J. Modi. «MOVING SURFACE BOUNDARY-LAYER CONTROL: A REVIEW». In: *Journal of Fluids and Structures* 11.6 (Aug. 1997), pp. 627–663. doi: 10.1006/jfls.1997.0098.
- [17] J. Iversen. «The Magnus Rotor as an Aerodynamic Decelerator». In: *2nd Aerodynamic Deceleration Systems Conference*. 2nd Aerodynamic Deceleration Systems Conference. El Centro, CA, U.S.A.: American Institute of Aeronautics and Astronautics, Sept. 23, 1968. doi: 10.2514/6.1968-962.
- [18] Miles C. Miller. «Wind-Tunnel Measurements of the Surface Pressure Distribution on a Spinning Magnus Rotor». In: *Journal of Aircraft* 16.12 (Dec. 1979), pp. 815–822. doi: 10.2514/3.58609.
- [19] A Betz. «The "Magnus Effect" - the Principle of the Flettner Rotor». In: *NACA Technical Memorandums* 310 (Apr. 1925).
- [20] Krahn, Edgar. «Negative Magnus Force». In: *Journal of Aeronautical Sciences* 24.4 (Oct. 1955), pp. 377–378. doi: doi:10.2514/8.3568.
- [21] Sophocles J. Orfanidis. *Introduction to Signal Processing*. Prentice Hall Signal Processing Series. Englewood Cliffs, N.J: Prentice Hall, 1996. 798 pp.

-
- [22] Ronald Schafer. «What Is a Savitzky-Golay Filter? [Lecture Notes]». In: *IEEE Signal Processing Magazine* 28.4 (July 2011), pp. 111–117. doi: 10.1109/MSP.2011.941097.